Technology Transfer of As-Built and Preliminary Surveys Using GPS, Soft Photogrammetry, and Video Logging

Iowa DOT Project TR-446
CTRE Project 00-66

Sponsored by
the Iowa Department of Transportation
and the Iowa Highway Research Board

Iowa Department of Transportation

CTRE
Center for Transportation Research and Education

Iowa State University

Final Report • May 2002

Technology Transfer of As-Built and Preliminary Surveys Using GPS, Soft Photogrammetry, and Video Logging

Abstract

This research involved two studies: one to determine the local geoid to obtain mean sea level elevations from a global positioning system (GPS) to an accuracy of ±2 cm, and the other to determine the location of roadside features such as mile posts and stop signs for safety studies, geographic information systems (GIS), and maintenance applications, from video imageries collected by a van traveling at traffic speed.

Four phases of local geoid determinations were conducted for nine stations in Story County. The variation fluctuated with time and the mean of all three had standard errors of less than ±2 cm. It was noted that the variations in local geoid may be due to motion of the axis of rotation of the earth. A need for a fixed-height antenna for all stations was indicated. It was also found that two sessions of observation can be used to detect blunders. It is recommended that the variation of local geoid over a long period of time, about 4–18 years, be studied so as to determine the validity of the moving average.

A video logging van capture imageries at three test sites: Grand Avenue, an urban site; EDM baseline, a rural site; and US 30 in Nevada, a freeway, at 55 mph. Evaluation of the data showed that the roadside feature location can be determined with relative accuracy better than 10 cm and absolute accuracy of ±2 m, depending on the global positioning system. The method developed was used to determine the state plane coordinates of mileposts and anchor points located along a 14-mile portion of US 30 from Ames to Nevada, Iowa. This information can be used in GIS and maintenance applications, as well as in safety studies. It is recommended that the Iowa Department of Transportation update the video logging van with a kinematic carrier phase GPS and conduct research with automatic data capture and by creating virtual roads.

The opinions, findings, and conclusions expressed in this publication are those of the authors and not necessarily those of the Iowa Department of Transportation.

CTRE’s mission is to develop and implement innovative methods, materials, and technologies for improving transportation efficiency, safety, and reliability while improving the learning environment of students, faculty, and staff in transportation-related fields.

Technology Transfer of As-Built and Preliminary Surveys Using GPS, Soft Photogrammetry, and Video Logging

Iowa DOT Project TR-446
CTRE Project 00-66

Principal Investigator
Kandiah Jeyapalan
Professor of Civil and Construction Engineering, Iowa State University

Co-Principal Investigator
Ed Jaselskis
Associate Professor of Civil and Construction Engineering, Iowa State University

Preparation of this report was financed in part
through funds provided by the Iowa Department of Transportation
through its research management agreement with the
Center for Transportation Research and Education.

Center for Transportation Research and Education
Iowa State University
2901 South Loop Drive, Suite 3100
Ames, Iowa 50010-8632
Telephone: 515-294-8103
Fax: 515-294-0467
www.ctre.iastate.edu

Final Report • May 2002

Table of Contents

EXECUTIVE SUMMARY ix

INTRODUCTION 1

Development of the Work Plan 1
Local Geoid Determination Tasks (GPS Measurements) 1
Position Determination Tasks (Video Logging and Soft Photogrammetry) 1

LOCAL GEOID DETERMINATION USING GPS 2

Introduction to Local Geoid Determination 2
Determination of Local Geoid for Story County Phase I 4
Determination of Local Geoid for Story County Phase II 8
Determination of Local Geoid for Story County Phase III 10
Estimation of Local Geoid for Story County Phase IV 14
Determination of Local Geoid for Story County Phase IV 16
Local Geoid Determination Conclusions and Recommendations 20

POSITIONING BY VIDEO LOGGING AND SOFT PHOTOGRAMMETRY 21

Introduction to Positioning 21
Methodology to Determine Position by Soft Photogrammetry 23
Methodology to Determine Position by Video Logging 29
Methodology to Locate Roadside Features at Nevada 36
Position Determination Conclusions and Recommendations 43

CONCLUSIONS AND RECOMMENDATIONS 45

ACKNOWLEDGMENTS 46

REFERENCES 47

APPENDIX A: PLAN FOR DEVELOPING LOCAL GEOID 49

APPENDIX B: PLAN FOR DEVELOPING OR SELECTING USER-FRIENDLY POSITIONING 51

APPENDIX C: INSTRUCTIONS FOR ESTABLISHING ELEVATION CONTROL BY GPS FOR REAL-TIME KINEMATIC GPS SURVEYS 55

List of Figures

Figure 1. Local Geoid 2
Figure 2. Location of Control (Story County) 4
Figure 3. Local Geoid Contour from G117 (contour interval of 0.5 cm) 7
Figure 4. Local Geoid Contour from DOT (contour interval of 0.5 cm) 7
Figure 5. Change in Local Geoid in Six Months (contour interval of 0.1 cm) 9
Figure 6. Geoid Variation with Time 12
Figure 7. Polar Motion of the Axis of Rotation of the Earth 13
Figure 8. Precession and Nutation Factors 13
Figure 9. Local Geoid Determined by Moving Average 19
Figure 10. Video Logging Van 21
Figure 11. Digital Video Image 22
Figure 12. Digital Orthophoto from Helicopter 22
Figure 13. Photo and Ground Coordinate System 23
Figure 14. Calibration Range with Control Points 25
Figure 15. Location of Video Images for Calibration 25
Figure 16. Ground Coordinate System 26
Figure 17. Test Sites (Story County) 30
Figure 18. EDM Baseline Theme 30
Figure 19. Grand Avenue Theme 31
Figure 20. Nevada Theme 32
Figure 21. Points Used at Grand Avenue 34
Figure 22. Points at Nevada 35
Figure 23. Event Theme Text File 36
Figure 24. Hotlinks Tool in ArcView 37
Figure 25. Location of Mileposts Determination Using Calib Program 38
Figure 26. ArcView Project 42
Figure 27. Anchor Points Added as a Separate Theme in ArcView 43

List of Tables

Table 1. Global Geoid 5
Table 2. Local Geoid Variation 6
Table 3. Differences Between Sessions 8
Table 4. Change in Local Geoid from G117 wrt 1999 Global Geoid 8
Table 5. Elevation and Geoid Undulation wrt 1999 for Day 282-01 10
Table 6. Elevations from the Three Phases 10
Table 7. Difference in Elevation Between 282-01 and 85-01 (G117 fixed during session A) 11
Table 8. Difference in Elevation Between 282-01 and 258-00 (G117 fixed during session A) ... 11
Table 9. Geoid Variation for the Three Phases 12
Table 10. Estimated Local Geoid for Story County Phase IV 15
Table 11. Difference in Elevation Between Session A and B of Day 78-02 (G117 fixed) 16
Table 12. Elevation and Geoid Undulation wrt 1999 for Day 78-02 16
Table 13. Difference in Elevation Between 282-01 and 78-02 (G117 fixed during session A) ... 17
Table 14. Difference in Elevation Between 78-02 and 85-01 (G117 fixed during session A) 17
Table 15. Difference in Elevation Between 78-02 and 258-00 (G117 fixed during session A) ... 18
Table 16. Difference Between Forecasted and Observed 18
Table 17. Moving Average Differences 19
Table 18. Interior Orientation Elements from Calibration 26
Table 19. Photo Coordinate Residuals 27
Table 20. Ground Coordinate Residuals 28
Table 21. Exterior Orientation Elements After Calibration 29
Table 22. Error at Checkpoints by Photogrammetric Triangulation 29
Table 23. Feature Location at EDM Baseline 33
Table 24. Error in Positioning by Video Logging (EDM baseline) 34
Table 25. Relative Error in Positioning by Video Logging (Grand Avenue) 35
Table 26. Error in Positioning by Video Logging (Nevada) 36
Table 27. Nevada Mileposts 41
Table 28. Anchor Point Results 42

EXECUTIVE SUMMARY

This research involves two studies: one to determine the local geoid to obtain mean sea level (m.s.l.) elevations from a global positioning system (GPS) to an accuracy of ±2 cm, and the other to determine the location of roadside features such as mile posts, stop signs, etc., for safety studies, geographic information systems (GIS), and maintenance applications, from video imageries collected by a van traveling at traffic speed.

In order to determine local geoid for Story County, nine benchmarks with known m.s.l. elevations distributed in both *x*, *y* directions covering the area were selected. Four phases of observations at six-month intervals were done. The first phase showed that the maximum variation of the local geoid is about 9 cm, suggesting the need for a local geoid to determine m.s.l. elevations from GPS. The first phase also showed that a local geoid contour from two base points can be used to determine m.s.l. elevations from GPS with accuracy better than ±2 cm.

Phases II, III, and IV were conducted to study the variation of the local geoid with time and find a method to forecast it. Phase II observations showed that there was a positive change in the local geoid over the six-month period. Phase III showed that the variation fluctuated with time and the mean of all three had standard errors of less than ±2 cm. This phase also showed that both Kalman filtering and moving average forecasted values agreed within ±2 cm. Phase III indicated the need for a fixed-height antenna for all the stations, and it was noted that the variations in local geoid may be due to motion of the axis of rotation of the earth.

Phase IV showed that the observed local geoid undulation agreed within ±2 cm with the forecasted values. The forecasted values by moving average were slightly better than those produced through Kalman filtering. The moving average of the last three phases local geoid undulation can be used to correct GPS observations for the next two years. Also, the difference between session A (morning four hours) and session B (afternoon four hours) agreed within ±2 cm, indicating the need for a fixed-height antenna and suggesting that two sessions of observation can be used to detect blunders.

The video logging van equipped with a high-resolution video camera, P-code phase GPS system, and inertial navigation system owned by the Iowa Department of Transportation (Iowa DOT) was calibrated using the special three-dimensional calibration range established at Iowa State University. Sequential imageries can then be used to determine locations on a local coordinate system without any control by constraining the interior and exterior orientation elements from calibration. The local coordinates can then be transformed to state plane coordinates using the camera locations determined by GPS. The van was used to capture imageries at three test sites: Grand Avenue, an urban site, at 25 mph; EDM baseline, a rural site, at 40 mph; and US 30 in Nevada, a freeway, at 55 mph. Evaluation of the data using both Calib, a research software, and SoftPlotter, a production software, showed that the roadside feature location can be determined with relative accuracy better than 10 cm and absolute accuracy of ±2 m, depending on the global positioning system. The coordinates determined have to be corrected for any systematic error caused by the GPS code phase system by having a control point every 15 miles. The method developed was used to determine the state plane coordinates of mileposts and anchor points

located along a 14-mile portion of US 30 from Ames to Nevada, Iowa. This information can be used in GIS and maintenance applications, as well as in safety studies.

It is recommended that the results of this research be presented at local, national, and international conferences. It is recommended that the variation of local geoid over a long period of time, about 4–18 years, be studied so as to determine the validity of the moving average. Finally, it is recommended that the Iowa DOT update the video logging van with a kinematic carrier phase GPS and conduct research with automatic data capture and creating virtual roads.

INTRODUCTION

Development of the Work Plan

The Iowa Highway Research Board (IHRB) approved the present project on March 31, 2000. In July 2000, the principal investigator (PI), Kandiah Jeyapalan, met with Ian MacGillivray of the Iowa Department of Transportation (Iowa DOT) and Mark Dunn of the IHRB to discuss the work plan. At this meeting, it was agreed to have a steering committee instead of the originally proposed advisory committee. The steering committee consisted of Alice Welch, John Whited, Bill Schuman, Sara Flanagan, John Smythe, and Bruce Brakke of the Iowa DOT; Don Callender, city engineer; Greg Parker, county engineer; and Jim Witt, county engineer. In September 2000, the Iowa State University (ISU) research team met with the steering committee, and in October 2000, they met with Iowa DOT officials to work out a detailed work plan. In January 2001, Mark Dunn and John Whited met with the PI and advised him to focus on determining the local geoid for Story County and on developing or selecting user friendly positioning by video logging and soft photogrammetry. Appendices A and B provide the work plan of this two-year project.

Local Geoid Determination Tasks (GPS Measurements)

Tasks 1–9 of the local geoid determination for Story County (see Appendix A) were completed as planned. This work indicates that a satisfactory local geoid will give elevation to ±2 cm absolute accuracy from global positioning system (GPS) measurements and that the local geoid is time dependent. Tasks 10–14 of the local geoid determination (Appendix A) will help to evaluate the change in local geoid over time and develop a Kalman filter technique to predict its value at any time.

Position Determination Tasks (Video Logging and Soft Photogrammetry)

Tasks 1–10 of the position determination by video logging and soft photogrammetry (see Appendix B) were completed as planned. It was found that the location of roadside features by video logging and soft photogrammetry can be determined to an absolute accuracy of ±1 m. This error is mainly due to the camera position error determined by the code phase kinematic GPS. The error due to soft photogrammetry is less than ±0.1 m. Tasks 11–13 of the position determination (see Appendix B) will help to evaluate the method over a 14-mile project along US 30 in Nevada, Iowa.

LOCAL GEOID DETERMINATION USING GPS

Introduction to Local Geoid Determination

GPS technology has developed rapidly during the last decade. It is now possible to determine locations with about ±2 cm accuracy in the global spherical coordinate system (φ, λ, h). The global spherical coordinate system gives height (h) above a reference ellipsoid. In engineering application, elevation (E) above mean sea level (m.s.l.) or a reference geoid is required. E can be obtained from

$$E = N + h,$$

where N is the geoid undulation. N is given by

$$Ng = U - U_0 = \Delta U = N(g_0 + \Delta g),$$

where U is the earth's gravitational potential measured at the point and U_0 is the potential of the reference geoid. U_0 is constant, and U, g, and N vary from point to point. Also,

$$g = g_0 + \Delta g$$

where g_0 is the computed gravity at the point on the reference ellipsoid, g is the measured gravity, and Δg is the gravity anomaly. See Figure 1.

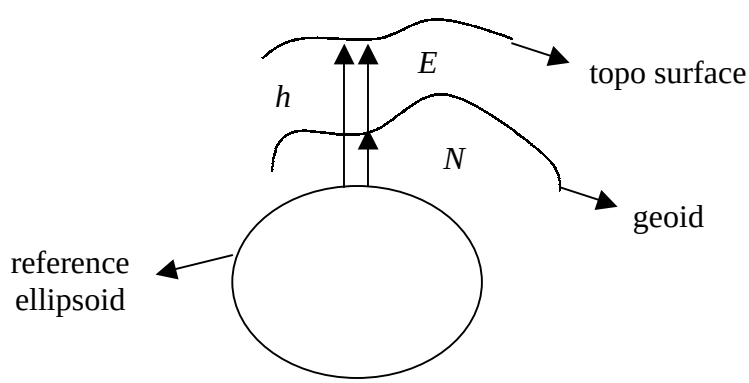

Figure 1. Local Geoid

Gravimeters that measure variation in gravity to a miligal can be used to measure Δg. The Δg value can then be used to determine parameters δC_{nm}, δS_{nm} from

$$\Delta g = \frac{GM}{R^2} \sum_{l=2}^{\infty} \sum_{m=0}^{l} (l-1)(\delta C_{lm} \cos m\lambda + \delta S_{lm} \sin m\lambda) P_{nm}(\cos \upsilon) \ ,$$

where $\nu = 90 - \varphi$, P_{nm} is Legandre's polynomial, and G, M, and R are constants of the reference ellipsoid. The parameters δC_{nm}, δS_{nm} can then be used to determine N from

$$N = R \sum_{l=2}^{\infty} \sum_{m=0}^{l} (l-1)(\delta C_{lm} \cos m\lambda + \delta S_{lm} \sin m\lambda) P_{nm}(\cos \upsilon)$$ (Torge, 1991, p. 154).

Gravity anomalies, Δg, are measured on a global scale on the ground and ocean. Satellite geodesy is used to determine Δg over the ocean and inaccessible locations on the ground. N can be determined directly by using precise geodetic leveling (E), GPS observations (h), and the equation

$$E = N + h,$$

where N is the geoid undulation.

Unfortunately, precise geodetic leveling is not available globally. Therefore, the National Geodetic Surveys (NGS) use a combination of precise leveling and gravity anomalies to predict the geoid undulation.

The earth's gravitational potential at a point varies with the location of the celestial bodies, the direction of the axis of rotation of the earth, and variation of material underneath and around the point. Thus, geoid undulation can be separated into two components: global (N_G) and local (N_L). Thus,

$$N = N_G + N_L.$$

NGS determines N_G periodically using 180 x 180 parameters of δC_{nm}, δS_{nm}, the latest available Δg, and E. The realistic accuracy of N_G is about ±10 cm. N_L has to be determined to an accuracy of ±2 cm to give a relative accuracy of ±2 cm in N. Past research efforts (Jeyapalan et al., 1991) by the research team indicate that N_L can be determined accurately for an area if

1. the error in N_G for the area is not greater than ±10 cm, and
2. at least six benchmarks (BM) with known geodetic leveling elevations (E) evenly distributed in X, Y directions are available.

Determination of Local Geoid for Story County Phase I

Using the Story County High Accuracy Reference Network (HARN) for Iowa, eight points—1370 (G301), G601, G605, G499, G117, 6 (G506), Ro1 (G001), and DOT distributed in *X*, *Y*—were selected (see Figure 2). Elevations of points G506, G001, and DOT were determined by three-wire leveling from nearby a first-order BM.

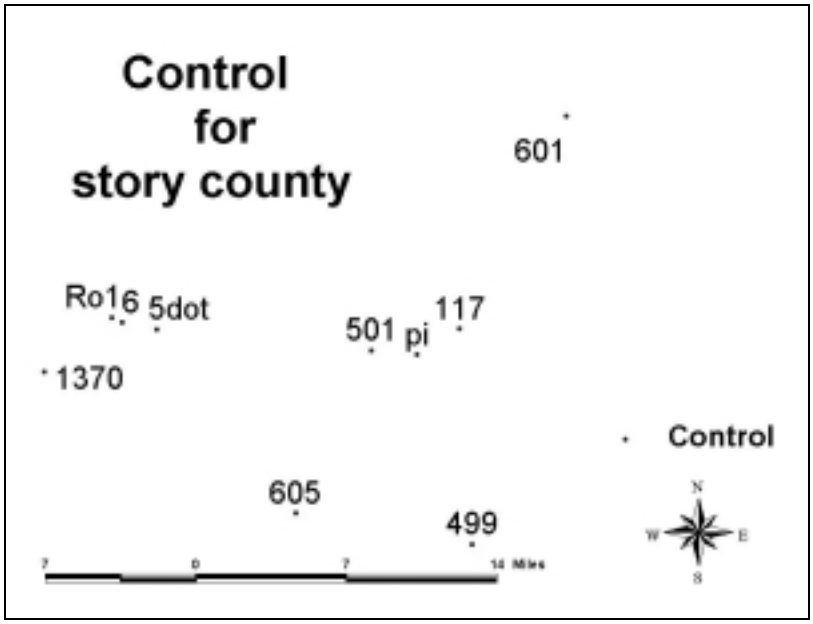

Figure 2. Location of Control (Story County)

Points G501 and PI (G017) are checkpoints. The approximate elevation of G501 is known. The difference in elevation between G501 and PI is determined by third-order leveling. In a typical preliminary survey, points G501 and PI will serve as the beginning and ending controls. Their geodetic elevations have to be determined by running three-wire level lines between the two closest control points, G117 and DOT. Considerable time and effort can saved if their elevations can be determined by two-hour GPS simultaneous observations from points G117 and DOT. However, this requires an N_L with sufficient accuracy.

N_L varies from point to point. Therefore, a function has to be developed to obtain its value. N_L may also vary with time. If it does, then a Kalman filtering technique has to be developed for predicting N_L at the time of the project.

NGS determines N_G periodically; it can be downloaded from the Internet. Table 1 shows the N_G values for 1996 and 1999 at the control points. The differences in N_G over the three years is about 3 cm, indicating that the geoid may vary at about 1 cm/year. In order to evaluate the change in N_L over the area, it is proposed that repeated GPS measurements be taken every six months over a period of two years.

Table 1. Global Geoid

Station	1996 Global Geoid	1999 Global Geoid	Difference
DOT	-29.305	-29.349	-0.044
G601	-29.965	-30.000	-0.035
G605	-30.542	-30.566	-0.024
G301	-29.140	-29.182	-0.042
G117	-30.272	-30.299	-0.027
G501	-30.106	-30.133	-0.027
G001	-29.079	-29.119	-0.040
G506	-29.141	-29.182	-0.041
G499	-30.949	-30.973	-0.024
G017	-30.251	-30.277	-0.026

GPS observations were collected on September 14, 2000 (hereafter day 258-00), except those for point PI (G017), which were collected on November 6, 2000 (hereafter day 310-00) (see Senthil Kumar and Patterson, Phase I, 2001). In order to eliminate any blunders due to the multi-path of the GPS signal, etc., two sessions, A and B, of 2.5 hours each of GPS observations were completed. The processing of the data was done using PRISM and SOLUTIONS software. SOLUTIONS uses default temperature and pressure values for atmospheric correction. PRISM has the option to compute with and without temperature and pressure values. Appendix B shows that processing A and B sessions with temperature and pressure do not give consistent results indicating the presence of some bug in the software. We propose to use the software supported by NGS to check the validity of the temperature and pressure corrections. However, our results (Senthil Kumar and Patterson, Phase I, 2001) indicated that SOLUTIONS (L1 and L2) gives consistent results that can be used in this study. Table 2 gives the local geoid, N_L, using the L1 carrier, from DOT and G117 with N_G of 1999. The differences in local geoid from both points are satisfactory as the reference values of the points are from an earlier adjustment, except at PI, where observations were taken for only one two-hour session and on a different date, 310-00. The multi-path of the GPS signal at DOT due to nearby construction activities on 310-00, is probably the cause of the difference.

Table 2 indicates a variation of about 9 cm in local geoid, which has to be corrected to determine the elevation with ±2 cm accuracy. Using the local geoid values at the control points, the values at the checkpoint G501 and PI can be obtained either by drawing local geoid contours or fitting a function

$$N_L = ax^2 + by^2 + cxy + dx + ey + f \ ,$$

where *a*, *b*, *c*, *d*, *e*, and *f* are parameters that can be computed by least squares using the eight control points.

Table 2. Local Geoid Variation

Station	Date	Local Geoid wrt 1999 from DOT	Local Geoid wrt 1999 from G117	Difference
G601	258-00	0.307	0.302	0.005
G605	258-00	0.254	0.232	0.022
G017	310-00	0.4743	0.3313	*0.143*
G301	258-00	0.367	0.33	0.037
G117	258-00	0.311	0.27	0.041
G501	258-00	0.364	0.324	0.04
G001	258-00	0.365	0.32	0.045
G506	258-00	0.347	0.306	0.041
G499	258-00	0.339	0.278	0.061
DOT	258-00	0.343	0.302	0.041

Using local geoid contours (in Appendix A) shown in Figures 3 and 4 the N_L for G501 from point G117 is 0.275 and from point DOT is 0.315. Thus, elevation of G501 (using the 258-00 observation) from point G117 by applying the local geoid correction is given by

$$E_{501} = E_{117} + \Delta h_{\mathrm{GPS}} + N_{117} - N_{501} - N_L = 273.775 + 30.113 - 0.275 = 303.613.$$

Similarly, the elevation of G501 from point DOT is given by

$$273.815 + 30.113 - 0.315 = 303.613,$$

which agrees exactly with the elevation from point G117, thereby providing a check and indicating a zero misclosure. This indicates that the local geoid gives satisfactory elevations agreeing with the approximate value of 303.583. The difference of 3 cm may be due to the fact that G501 elevation is on 1929 datum rather than the 1988 vertical datum used in the control points.

Similarly, elevation of PI from G117 (310-00, observation) is given by

$$269.865 + 30.277 - 0.272 = 299.87.$$

Thus, the difference in elevation between G501 and PI by GPS is

$$303.613 - 299.87 = 3.743 \text{ m},$$

compared with the difference by third-order leveling,

303.583 - 299.8107 = 3.7723 m.

The difference of 2 cm is an acceptable misclosure for a third-order level. Also, this difference may be due to a change in local geoid over the two months and or due to normal GPS instrument setup error. A better determination of the local geoid can be obtained by using a least squares, which may also help eliminate any systematic error.

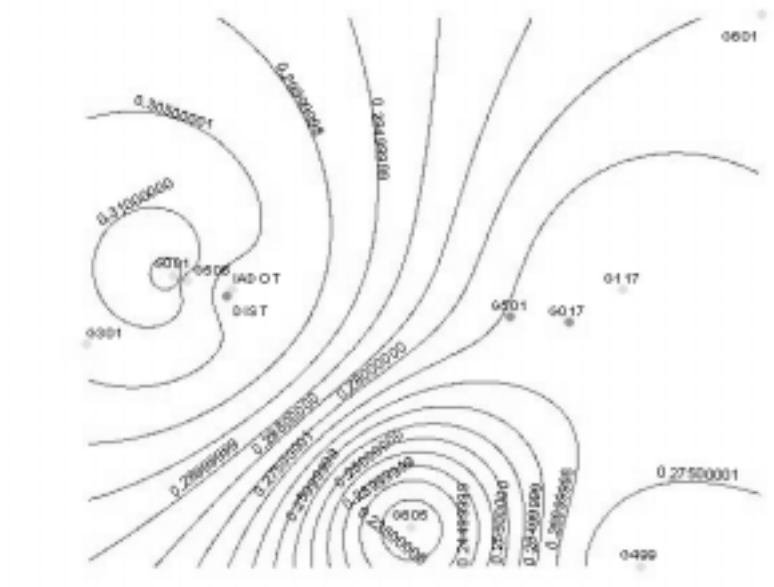

Figure 3. Local Geoid Contour from G117 (contour interval of 0.5 cm)

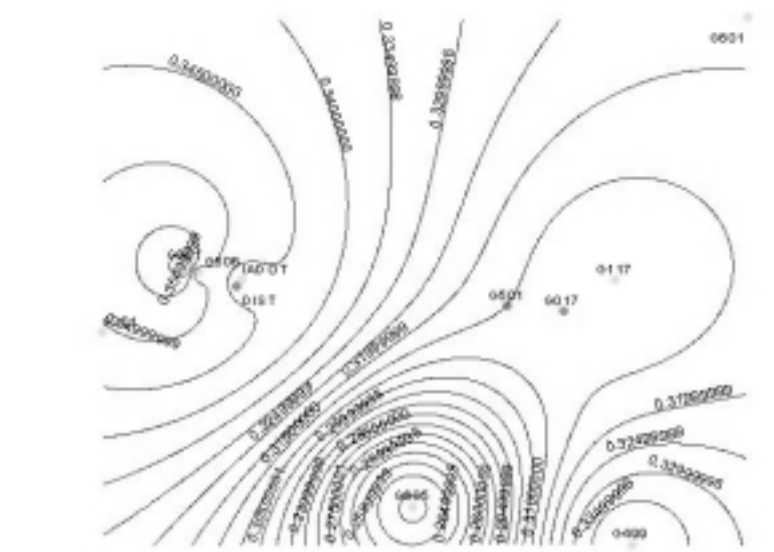

Figure 4. Local Geoid Contour from DOT (contour interval of 0.5 cm)

Determination of Local Geoid for Story County Phase II

Two four-hour sessions of GPS observations on March 26, 2001, (hereafter day 85-01) and March 27, 2001, (hereafter day 86-01) were completed at all the stations (see Senthil Kumar and Patterson, Phase II, 2001). Table 3 shows the differences in ellipsoidal height obtained by GPS at all the stations using the SOLUTIONS software. The differences indicate that virtually all differences are less than three times expected standard error of 2 cm.

Table 3. Differences Between Sessions

Station G117 to Station	85-01 Elev.	86-01 Elev.	Diff. 85-01 - 86-01	Solution A (258-00 a.m.)	Solution B (258-00 p.m.)	Diff. A - B	Diff. 85-01 - A	Diff. 86-01 - B
DIST	244.041	244.089	-0.048	—	—	—	—	—
G001	264.426	264.472	-0.046	264.432	264.389	0.043	-0.006	0.083
G017	269.865	269.872	-0.007	269.865	—	—	—	—
G301	285.504	285.5	0.004	285.483	285.474	0.009	0.021	0.026
G499	232.193	232.186	0.007	232.186	232.177	0.009	0.007	0.009
G501	273.784	273.787	-0.003	273.776	273.754	0.022	0.008	0.033
G506	258.268	—	—	258.248	258.189	0.059	0.02	—
G601	299.881	299.862	0.019	299.869	299.885	-0.016	0.012	-0.023
G605	234.026	234.043	-0.017	234.027	233.988	0.039	-0.001	0.055
DOT	263.712	263.726	-0.014	263.702	263.676	0.026	0.01	0.05

Table 4 shows the change in local geoid from station G117. The changes in N_L over a six-month period are positive and small. Figure 5 shows the change in local geoid contours.

Table 4. Change in Local Geoid from G117 wrt 1999 Global Geoid

Station G117 to Station	258-00 Local Geoid	85-01 Local Geoid	Change in Six Months
G601	0.306	0.318	0.012
G605	0.224	0.223	-0.001
G017	0.331	0.3313	0
G301	0.349	0.37	0.021
G117	0.27	0.27	0
G501	0.325	0.333	0.008
G001	0.327	0.321	-0.006
G506	0.317	0.337	0.02
G499	0.265	0.272	0.007
DOT	0.303	0.313	0.01

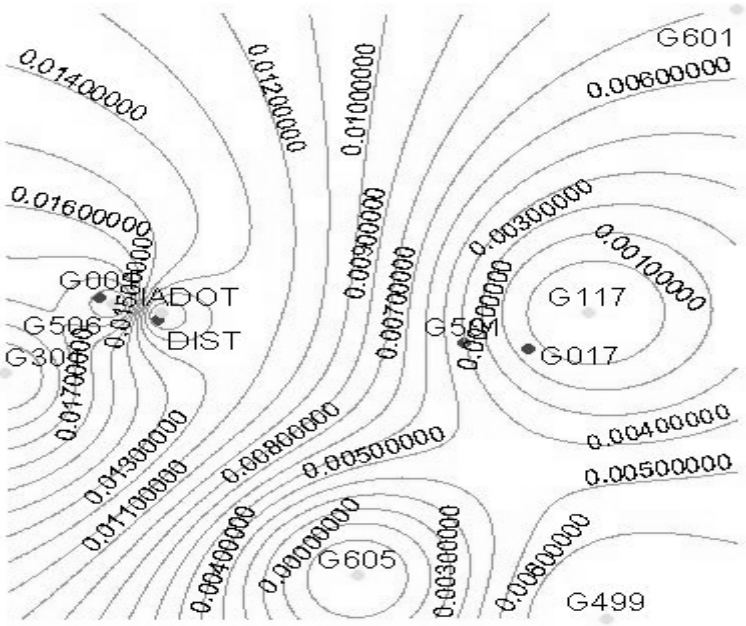

Figure 5. Change in Local Geoid in Six Months (contour interval of 0.1 cm)

Determination of Local Geoid for Story County Phase III

On October 9, 2001, (hereafter day 282-01) two four-hour sessions (A and B) of global positioning system (GPS) observations were conducted at all the stations (see Ramesh, Phase III, 2001).

Table 5 shows the ellipsoidal height and the local geoid obtained by GPS at all the stations using the SOLUTIONS software for session A. The differences between sessions A and B indicated that virtually all differences are less than three times the expected standard error of 2 cm, except at DOT, which was about 6.5 cm. Further investigation revealed that this may be due to construction activities close to the station DOT, as well as due to the fact that a fixed-height antenna was not used at this station. However, the session A elevations are consistent with the earlier observations (see Table 6) and are therefore used in this study.

Table 5. Elevation and Geoid Undulation wrt 1999 for Day 282-01 (G117 fixed during session A)

Station	282-01 Elevation	Geoid Undulation wrt 1999 for Day 282-01
G117 fixed	277.496	-0.270
DOT	263.713	-0.314
G601	299.837	-0.274
G499	232.229	-0.308
G605	234.052	-0.249
G301	285.476	-0.342
G501	273.777	-0.326
(G001) 7263	264.402	-0.297
(G506) 1165	258.216	-0.285
(G017) 7373	269.881	-0.3473

Table 6. Elevations from the Three Phases

Station	258-00 Elevation	85-01 Elevation	282-01 Elevation
G117	277.496	277.496	277.496
DOT	263.702	263.712	263.713
G601	299.869	299.881	299.837
G499	232.186	232.193	232.229
G605	234.027	234.026	234.052
G301	285.483	285.504	285.476
G501	273.776	273.784	273.777
G001	264.432	264.426	264.402
G506	258.248	258.268	258.216
G017	269.865	269.865	269.881

Tables 7 and 8 indicate that the standard error of the differences between Phase III and the first two phases are larger than 2 cm, suggesting that the geoid model developed using either Phase I or Phase II is not acceptable for Phase III observations.

Table 7. Difference in Elevation Between 282-01 and 85-01 (G117 fixed during session A)

Station	**Difference in Elevation 282-01 - 85-01**
G117 fixed	0
DOT	0.001
G601	-0.044
G499	0.036
G605	0.026
G301	-0.028
G501	-0.007
(G001) 7263	-0.024
(G506) 1165	-0.052
(G017) 7373	0.016
1__ (DIST)	-0.004
Mean	-0.008444444
Standard error	0.030895433

Table 8. Difference in Elevation Between 282-01 and 258-00 (G117 fixed during session A)

Station	**Difference in Elevation 282-01 - 258-00**
G117 fixed	0
DOT	0.011
G601	-0.032
G499	0.043
G605	0.025
G301	-0.007
G501	0.001
(G001) 7263	-0.03
(G506) 1165	-0.032
(G017) 7373	0.016
Mean	-0.000555556
Standard error	0.027032902

However, Table 9 shows that the mean of the phases gives a standard error of the differences less than 2 cm, and Figure 6 shows the variation of the geoid with time.

Table 9. Geoid Variation for the Three Phases

Station	Mean	Mean - 258-00	Mean - 85-01	Mean - 282-01
G117	277.496	0	0	0
DOT	263.709	-0.007	0.003	0.004
G601	299.8623333	0.006667	0.018667	-0.02533
G499	232.2026667	-0.01667	-0.00967	0.026333
G605	234.035	-0.008	-0.009	0.017
G301	285.4876667	-0.00467	0.016333	-0.01167
G501	273.779	-0.003	0.005	-0.002
G001	264.42	0.012	0.006	-0.018
G506	258.244	0.004	0.024	-0.028
G017	269.8703333	-0.00533	-0.00533	0.010667
Mean	—	-0.0022	0.0049	-0.0027
Standard deviation	—	0.008206	0.011662	0.018041

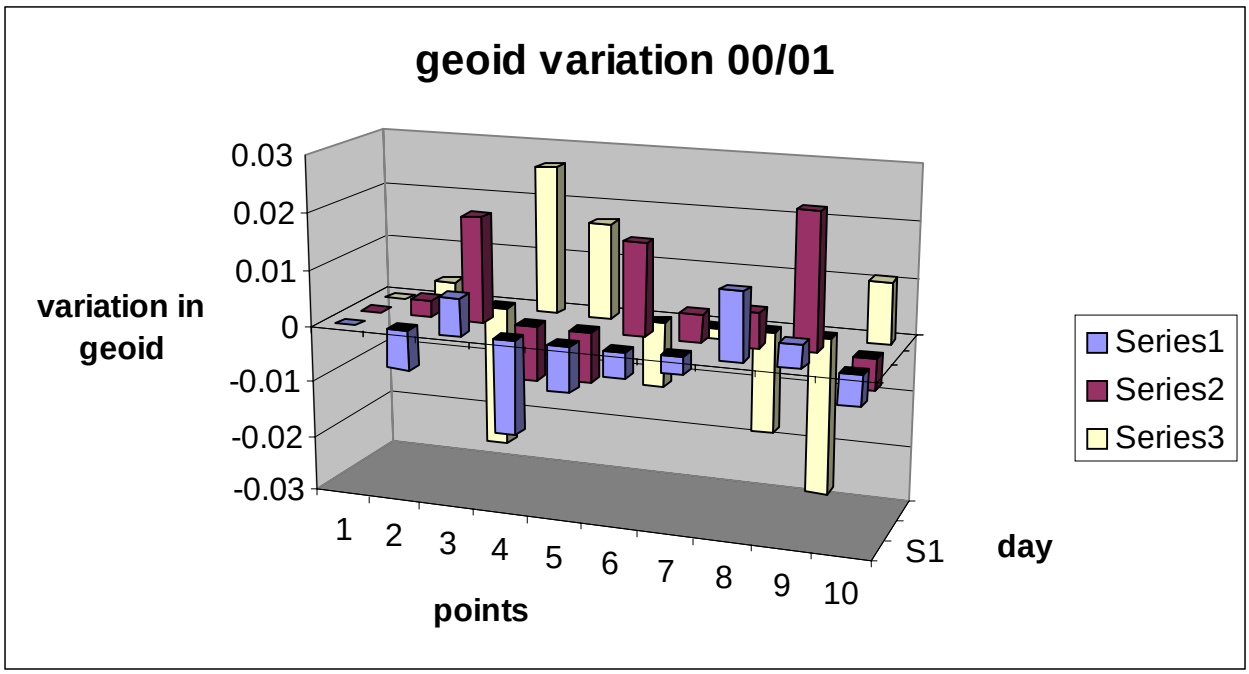

Figure 6. Geoid Variation with Time

The variation in geoid with time suggests that this may be due to polar motion of the axis of rotation of the earth caused by precession and nutation (see Figures 3.2 and 4.3. from Torge, reproduced here as Figures 7 and 8, respectively) and Chandler effects. Additional factors include the movement of masses under the surface of the earth, such as crustal movement, and the seasonal water table. The mass movement will change the location of the center of mass of the earth, which in turn will affect the GPS elevation. It has to be noted that the inertial axis of rotation of the earth changes with time, where as WGS 84 is a coordinate system fixed in time,

Julian day 0, 1984. Thus, it can be concluded that GPS or ellipsoidal elevation is time dependent and the mean sea level (m.s.l.) elevation or orthometric elevation is on the inertial system and independent of time. Thus, the local geoid will change with time.

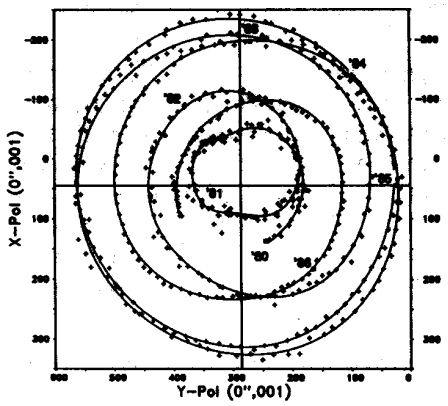

Fig. 3.2. Polar motion 1980 to 10/1986, solution ERP (DGFI I) 87L02, from SCHNEIDER (ed.) 1990

Figure 7. Polar Motion of the Axis of Rotation of the Earth

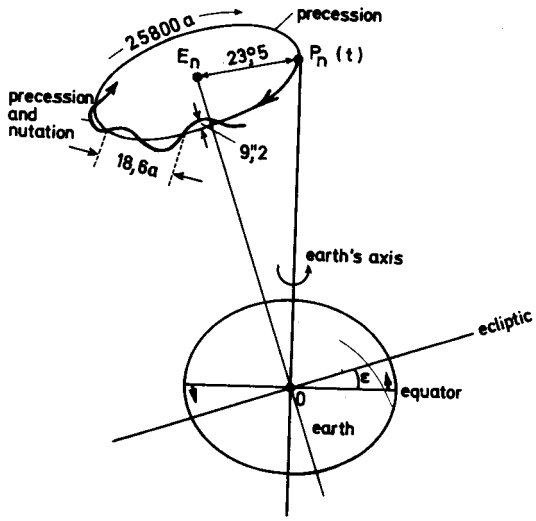

Fig. 4.3. Precession and nutation

Figure 8. Precession and Nutation Factors

Estimation of Local Geoid for Story County Phase IV

The local geoid difference, N, can be predicted using the equation

$$N_T = N_{To} + vt + \tfrac{1}{2}at^2, \tag{1}$$

where $t = T - To$ is the interval of time, v is the velocity, and a is the acceleration. Thus, using the three phases of observations (258-00, 85-01, and 282-01), the parameters N_{To}, v, and a can be calculated and geoid differences for the fourth phase can be predicted.

Since the mean or the moving average gives standard errors less than 2 cm, it can be used to predict geoid differences for the Phase IV.

The Kalman filtered state vector is given by

$$\hat{X}_k(+) = \hat{X}_k(-1) + K_k(Z_k - H_k \hat{X}_k(-1)),$$

where

$$\hat{X}_k(+)$$

is the filtered state vector and

$$\hat{X}_k(-)$$

is the predicted state vector. The Kalman gain matrix, K_k, is given by

$$K_k = P_{k-1}(-1)H_k^T(H_k P_k(-1)H_k^T + R_k)^{-1},$$

where P_k(-) is the covariance matrix for the predicted state vector and P_k(+) is the covariance for the filtered state vector. The covariance matrix for the predicted state vector is given by

$$P_k(-1) = \Phi_{k-1}P_k(+1)\Phi_{k-1}^T + Q_k,$$

where Q_k is the covariance of the error in X_k. The predicted state vector is given by

$$\hat{X}_k(-1) = \Phi_{k-1}\hat{X}_{k-1}(+1) = \begin{pmatrix} 1 & \Delta t \\ 0 & 1 \end{pmatrix} \begin{bmatrix} N_{k-1} \\ a_{k-1} \end{bmatrix}.$$

H_k is the measurement matrix, and Z_k is the measurement vector. With initial estimates for P_0, R_k, and Q_k, the values for $X_k(+)$ can be computed (see Cederholm, 2000).

Table 10 gives the predicted, moving average, and Kalman filtered values for the Phase IV. The table shows that the predicted value using the equation (1) does not agree with the other two. However, the moving average agrees with the Kalman filtered values, suggesting that moving average is an acceptable method to forecast the geoid undulation.

Table 10. Estimated Local Geoid for Story County Phase IV

Station	Velocity	Acceleration	Predicted Geoid Difference	Moving Average Geoid Difference	Kalman Geoid Difference
G117	0	0	-0.27	-0.27	-0.27
DOT	-0.029	0.036	-0.306	-0.31	-0.32
G601	-0.08	0.224	-0.174	-0.299	-0.317
G499	0.015	-0.116	-0.373	-0.282	-0.3235
G605	0.029	-0.108	-0.302	-0.232	-0.256
G301	-0.091	0.196	-0.265	-0.35367	-0.368
G501	-0.031	0.06	-0.304	-0.328	-0.339
G001	-0.006	0.072	-0.255	-0.315	-0.29705
G506	-0.112	0.288	-0.161	-0.313	-0.3292
G017	0.016	-0.064	-0.3793	-0.33663	-0.338

Determination of Local Geoid for Story County Phase IV

In March 19, 2002, (hereafter day 78-02) two four-hour sessions (A and B) of GPS observations were conducted at all the stations (see Ramesh, 2002, p. 78). Table 11 gives the computed elevations for the two sessions and the differences. The largest difference is less than 3 cm, indicating that both observations are satisfactory. The main reason for this agreement is that fixed-height antennae were used at all stations, unlike in the other phase observations.

Table 11. Difference in Elevation Between Session A and B of Day 78-02 (G117 fixed)

Station	78-02 Session A Elevation	78-02 Session B Elevation	Difference in Elevation 78-02 Session A - Session B
DOT	263.717	263.708	0.009
G601	299.85	299.833	0.017
G499	232.234	232.246	-0.012
G605	234.051	234.061	-0.01
G301	285.453	285.48	-0.027
G117 fixed	277.496	277.496	0
G501	273.773	273.768	0.005
(G001) 7263	264.41	264.396	0.014
(G506) 1165	258.244	258.237	0.007
(G017) 7373	269.877	269.87	0.007

Table 12 gives the difference in the geoid undulation for Phase IV. Tables 13–15 show the standard error of the differences between phases or the change increases with time. The differences between day 78-02 and day 258-00 are all positive, the largest being 9 cm, which clearly indicates that the geoid observed on day 258-00 is not acceptable for 78-02.

Table 12. Elevation and Geoid Undulation wrt 1999 for Day 78-02 (G117 fixed during session A)

Station	78-02 Elevation	Geoid Undulation wrt 1999 for Day 78-02
DOT	263.717	-0.318
G601	299.85	-0.287
G499	232.234	-0.313
G605	234.051	-0.248
G301	285.453	-0.319
G117 fixed	277.496	-0.27
G501	273.773	-0.322
(G001) 7263	264.41	-0.305
(G506) 1165	258.244	-0.313
(G017) 7373	269.877	-0.3433

Table 13. Difference in Elevation Between 282-01 and 78-02 (G117 fixed during session A)

Station	Difference in Elevation 78-02 - 282-01
DOT	0.06
G601	0.002
G499	0.011
G605	0.005
G301	0.063
G117 fixed	0
G501	0.001
(G001) 7263	0.013
(G506) 1165	0.029
(G017) 7373	-0.004
Mean	0.019727273
Standard error	0.024154051

Table 14. Difference in Elevation Between 78-02 and 85-01 (G117 fixed during session A)

Station	Difference in Elevation 78-02 - 85-01
DOT	0.005
G601	-0.031
G499	0.041
G605	0.025
G301	-0.051
G117 fixed	0
G501	-0.011
(G001) 7263	-0.016
(G506) 1165	-0.024
(G017) 7373	0.012
Mean	-0.001818182
Standard error	0.02802434

Table 15. Difference in Elevation Between 78-02 and 258-00 (G117 fixed during session A)

Station	Difference in Elevation 78-02 - 258-00
DOT	0.0706
G601	0.0868
G499	0.0602
G605	0.0686
G301	0.0175
G117 fixed	0
G501	-0.0383
(G001) 7263	0.041
(G506) 1165	0.092
(G017) 7373	—
1___(DIST)	—
Mean	0.044266667
Standard error	0.043489798

Table 16 shows the differences between observed Phase IV values and the expected values by moving average and Kalman filtering from Table 10. The standard error of the differences for both the moving average and Kalman filtering are less than 2 cm. The differences indicate that the moving average is better than the Kalman technique and that the maximum difference is less than 4 cm, which would be less than half if we used Phase I observations.

Table 16. Difference Between Forecasted and Observed

Station	Kalman - Moving Average	Observed (78-02)	Kalman - Observed	Moving Average - Observed
G117	—	—	—	—
DOT	-0.01	-0.318	-0.002	0.008
G601	-0.018	-0.287	-0.03	-0.012
G499	-0.0415	-0.313	-0.0105	0.031
G605	-0.024	-0.248	-0.008	0.016
G301	-0.01433	-0.319	-0.049	-0.03467
G501	-0.011	-0.322	-0.017	-0.006
G001	0.01795	-0.305	0.00795	-0.01
G506	-0.0162	-0.313	-0.0162	0
G017	-0.00137	-0.343	-0.00803	0.006367
Mean	-0.01316	—	-0.01475	-0.00014
Standard error	0.015189	—	0.015633	0.017648

Table 17 shows that the moving average of the latest three observations—Phases IV, III, and II, and their differences with the previous three observations—Phases III, II, and I. The differences are less than 2 cm and are random; therefore, this moving average could be useable for about two

years. However, a long-term study may indicate the frequency at which this local geoid has to be replaced. It is to be noted that tide gauge readings are taken over a period of 18 years, the period of nutation effect on the polar motion (see Figures 7 and 8). Figure 9 shows the moving average contour with a 5-mm interval, which can be used to estimate the local undulation at any point in the area during 2002–2003.

Table 17. Moving Average Differences

Point	Moving Average	Change in Moving Average
G117	-0.27	0
DOT	-0.315	-0.005
G601	-0.293	0.006333
G499	-0.2976	-0.016
G605	-0.24	-0.008
G301	-0.3436	0.01
G501	-0.327	0.001
G001	-0.3076	0.007333
G506	-0.31166	0.001333
G017	-0.3405	-0.0039

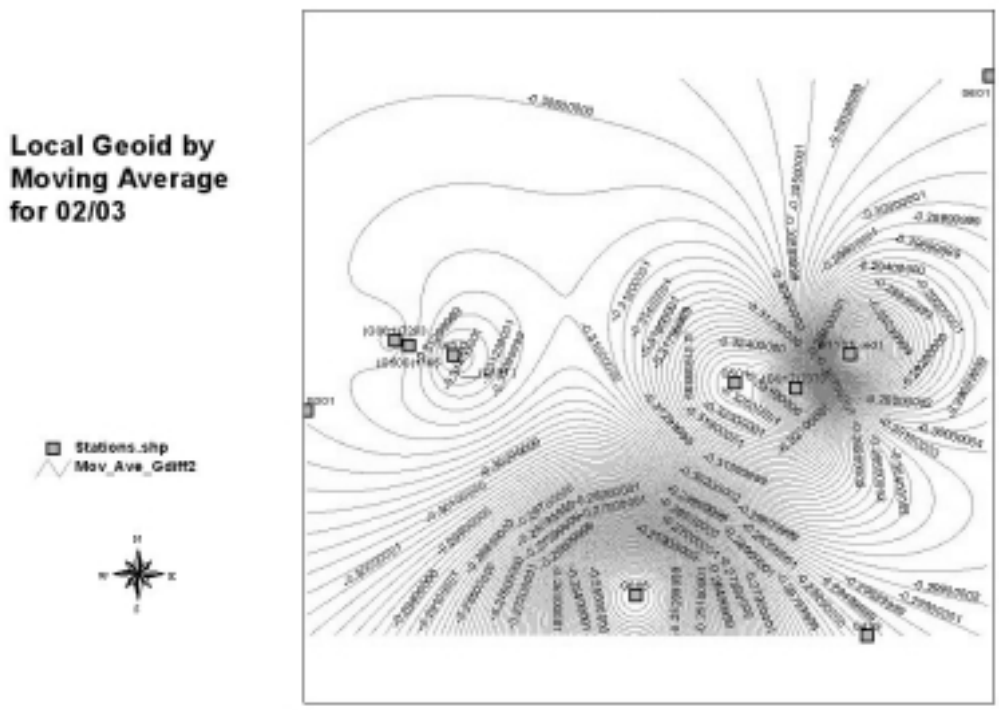

Figure 9. Local Geoid Determined by Moving Average

Local Geoid Determination Conclusions and Recommendations

The local geoid, N, is needed to get mean sea elevation, E, from GPS height, h, to an accuracy of ±2 cm. If at least eight benchmarks of known mean sea elevation are available in an area, then GPS observations can be made at all these stations simultaneously and the geoid differences from any one of these stations can be computed by processing the data as vectors from that station. If the geoid differences are less than 10 cm, then the geoid contours by spline or other standard methods, for which software is easily available, can be developed and the geoid difference for any point of interest can then be interpolated. However, if the geoid differences are larger than 10 cm, then after checking for any blunders, the area may have to be split into two or more sections and a separate local geoid for each section have to be developed.

It is important that the locations of BMs should be distributed in x, y direction so that the contours are representative of the area. In order to get mean sea level elevation at a point of interest from GPS, it is better to get the computed values from two points and adopt the mean if they agree within 2 cm. Thus,

$$E = [(h_1 + N_1) + (h_2 + N_2)]/2 \text{ and } |(h_1 + N_1) - (h_2 + N_2)| \leq 2 \text{ cm.}$$

Since the local geoid varies with time, it is better to determine the values every six months and use the moving average, N_{mov}, of the three previous values for the next six months and so on. However, further research might prove that the average of three values may be satisfactory for two or more years. Figure 9 shows the moving average geoid contours from

$$N_{mov} = (N_{1t0} + N_{1t1} + N_{1t2})/3,$$

where t_0 = 85/01, t_1 = 282/01, and t_2 = 78/02, which can be used to interpolate local geoid for any point in the area during 2002–2003.

Detailed instructions for establishing elevation control for real-time kinematic (RTK) GPS projects is given in Appendix C.

POSITIONING BY VIDEO LOGGING AND SOFT PHOTOGRAMMETRY

Introduction to Positioning

Figure 10 shows the video logging van used by the Iowa DOT. The van is equipped with a side-looking (about five degrees) high-resolution digital camera, L1/L2 GPS receiver for kinematic applications, a distance measuring instrument (DMI), and a computer system for recording GPS information and storing the digital images. As the van travels along the road at traffic speed, the DMI controls the camera exposure to take video images every 25 feet. The position of the van at the time of every video image is determined by the post-processing kinematic GPS method using the base station receiver located at the Iowa DOT.

Figure 10. Video Logging Van

Figure 11 shows a typical video image. The problem is to determine the location of roadside features such as power poles, fence posts, marks on the road surface, etc., to required accuracy. It is easy to identify standing objects such as fence posts, telephone boxes, and power lines as both the scale and ground resolution are large, unlike in aerial photos. Figure 12 shows the orthophoto created from low-flying (300 feet above ground) soft photogrammetry (Jeyapalan et al., 1998). From a comparison of the two images, it is obvious that video logging image gives better imagery for identifying roadside features. However, it must be noted that creation of orthophotos from video logging is tedious and time consuming as the variation in *Z* (the direction of line-of-sight) is large compared with that from an aerial photograph.

Figure 11. Digital Video Image

Figure 12. Digital Orthophoto from Helicopter

Methodology to Determine Position by Soft Photogrammetry

If (X_G, Y_G, Z_G) is the ground location of a point and (x_p, y_p) is its location on the video image (see Figure 13), then by direct linear transformation (DLT) of the central projection (Jeyapalan et al., 1998),

$$x_p = \frac{m_{11}X_G + m_{12}Y_G + m_{13}Z_G + m_{14}}{m_{31}X_G + m_{32}Y_G + m_{33}Z_G + 1},$$
$$y_p = \frac{m_{21}X_G + m_{22}Y_G + m_{23}Z_G + m_{24}}{m_{31}X_G + m_{32}Y_G + m_{33}Z_G + 1}$$

where $m_{11} \ldots m_{33}$ are parameters that can be determined by having at least six control points for which (X_G, Y_G, Z_G) and (x_p, y_p) are known. If the parameters are known, then for any ground point that appears on two video images, the ground location (X_G, Y_G, Z_G) can be determined by measuring the image coordinates (x_p, y_p) on both video images. Software such as PhotoModeler (available on the Internet) can be used to process these data. However, in video logging there are four video images for every 100 feet; therefore, we need at least six control points for every pair of video images used for locating roadside features. This is impractical even though the computation is straightforward.

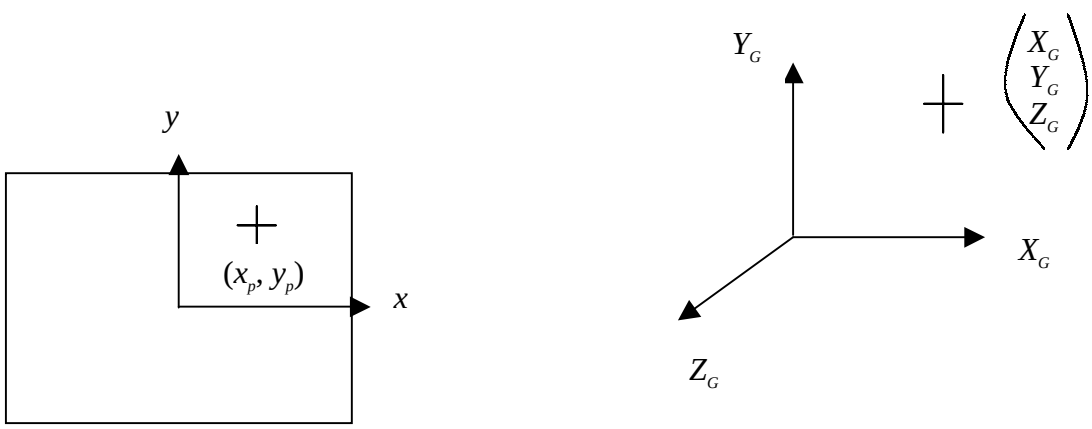

Figure 13. Photo and Ground Coordinate System

Alternatively, using the collinearity condition of the central projection (Jeyapalan et al., 1998), the equations are

$$x_p = -f\,\frac{a_{11}(X_G - X_0) + a_{12}(Y_G - Y_0) + a_{13}(Z_G - Z_0)}{a_{31}(X_G - X_0) + a_{32}(Y_G - Y_0) + a_{33}(Z_G - Z_0)},$$
$$y_p = -f\,\frac{a_{21}(X_G - X_0) + a_{22}(Y_G - Y_0) + a_{23}(Z_G - Z_0)}{a_{31}(X_G - X_0) + a_{32}(Y_G - Y_0) + a_{33}(Z_G - Z_0)}$$

where f is the principal distance between the lens and the video image plane in the digital camera, (X_0, Y_0 , Z_0) is the location of the camera in the ground system, and 0_{11} … a_{33} are parameters depending on the orientation (κ, φ, ω) of the camera to the ground system.

In video logging, the location of the camera for every image is determined by GPS. The orientation angles φ, ω can be determined from the locations of sequential video camera and the orientation angle κ together with (X_G, Y_G, Z_G) can be determined from four or more equations obtained from two or more photo coordinates measured on two or more sequential video images.

The pixel values of a point can be easily measured on the video image displayed on a PC. These pixel values P_x, $P_{y,}$ must be corrected for lens distortion and location of principal point x_0, y_0 to give x_p, y_p from

$$x_p = p_x - x_0 + p_x(k_1 + k_2 r^2 + k_3 r^4) + \{p_1(r^2 + 2p_x^2) + 2p_2 p_x p_y)\{1 + p_3 r^2\}$$
$$y_p = p_y - y_0 + p_y(k_1 + k_2 r^2 + k_3 r^4) + \{p_1(r^2 + 2p_y^2) + 2p_2 p_x p_y)\{1 + p_3 r^2\},$$

where $r^2 = p_x^2 + p_y^2$.

The principal distance, correction due to lens distortion, origin of the photo, and the initial orientation angles for simultaneous least squares processing of the data can be obtained by proper calibration of the system (see Bhagawati and Patterson, Dynamic Calibration, 2001).

A calibration range (see Figure 14) was set up so that sufficient control points are located with even distribution in X, Y and in Z. This will enable us to determine the interior orientation elements (x_0, y_0, f, k_1, k_2, k_3, p_1, p_2, p_3) without any correlation among themselves and with the exterior orientation elements (X_0, Y_0 , $Z_{0,}$ κ, φ, ω).

The site was selected so that the video van can easily be driven in front of the test range and video images taken at 25, 38, 50, and 60 feet from the range (see Figure 15). The ground coordinates of the targets were determined to an accuracy of ± 3 cm using a Geodimeter 400 total station. Initial pixel values were measured on the digital image, which were then shifted to the center of the image to give the pixel coordinates.

Figure 14. Calibration Range with Control Points

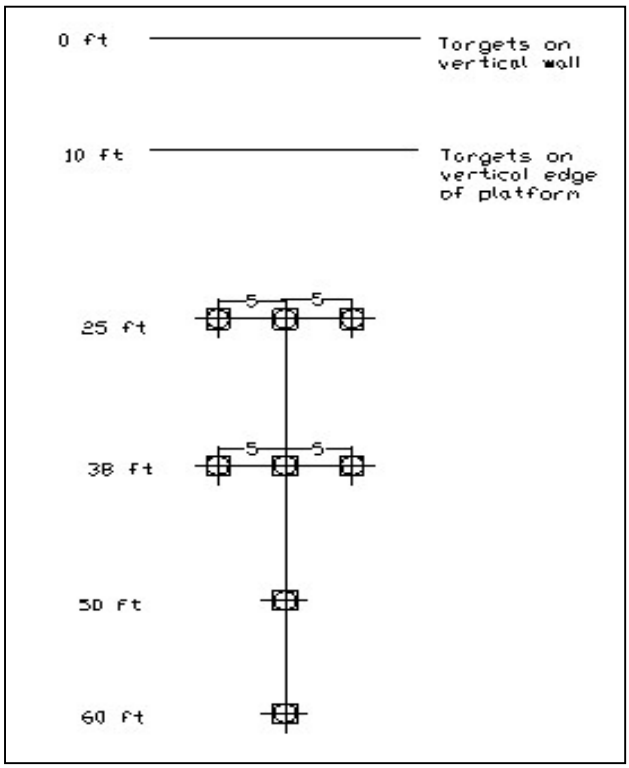

Figure 15. Location of Video Images for Calibration

The photo coordinates from the video images at 25, 38, and 60 feet from the wall, where the ground control targets are placed, together with the ground coordinates (see Figure 16) were simultaneously adjusted using the Calib software to determine x_0, y_0, f, k_1, k_2, k_3, p_1, p_2, p_3,κ, φ, and ω. Ground coordinates, pixel coordinates, and camera locations were constrained to a known accuracy, and light weights were assigned to interior orientation elements so as to give optimum solution and minimum standard error of unit weight. Table 18 shows that the resultant standard error of unit weight is 0.8. It also shows the interior orientation elements and their standard errors, which were satisfactory.

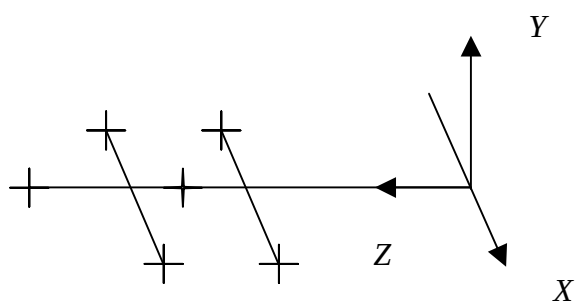

Figure 16. Ground Coordinate System

Table 18. Interior Orientation Elements from Calibration

ICYCLE = 3 VARIANCE = 8.28E-01 NDF = 129							
CAMERA CALIBRATION OF THE VIDEOLOG F 2000							
NO. OF PHOTOS 3							
NO. OF CONTROL POINTS 36							
DEGREES OF FREEDOM 129							
NO. OF CYCLES 3							
VARIANCE OF UNIT WEIGHT = 8.28E-01							
RESULTS							
INTERIOR ORIENTATION							
X	Y	F					
0.0424873	0.0081226	-1819.9934					
K1*1.00E-05	K2*10**-12	K3*10**-18	P1*1.00E-05	P2*10**-12	P3*10**-18		
0.001279	-0.002277	-0.000011	0.018948	0	0		
STD ERROR	0.91	0.91	0.91	0.00863	0.0148	0.00906	0.286

The final adjustment gave the residuals in the photo coordinates of less than 0.5 pixels (see Table 19) and ground coordinate residual of less than 0.3 m (see Table 20). These are satisfactory as the objective is to determine the location of the roadside features within 0.5 m.

Table 19. Photo Coordinate Residuals

Residuals on Control Points (Photo Coordinate Units)						
S. No.	Point No.	X Coord.	Y Coord.	Z Coord.	Res. X	Res. Y
1	11	1.831	5.415	-7.637	-0.000945	0.000333
2	12	3.724	5.419	-7.637	-0.000566	0.000404
3	13	6.141	5.405	-7.642	-0.000197	0.000221
4	14	8.504	5.382	-7.655	-0.000015	-0.000081
5	15	10.627	5.436	-7.669	-0.000398	0.000751
6	21	3.008	4.812	-7.639	-0.000853	0.000375
7	22	4.388	4.812	-7.641	-0.000486	0.000359
8	23	6.127	4.803	-7.647	-0.000154	0.00026
9	24	7.844	4.794	-7.653	0.000008	0.000111
10	25	9.215	4.766	-7.664	0.000056	-0.000214
11	31	1.793	4.074	-7.586	-0.158509	-0.208739
12	32	3.013	3.793	-7.505	-0.224709	-0.215069
13	33	4.384	3.613	-7.636	-0.508089	-0.099599
14	34	6.139	3.796	-7.581	-0.31129	0.189664
15	35	7.89	3.806	-7.872	-0.219866	0.369809
16	36	9.267	3.793	-7.954	0.03543	-0.006485
17	37	10.643	4.004	-7.682	-0.00022	-0.000442
18	41	1.779	2.377	-7.552	-0.02417	-0.160649
19	42	3.006	2.368	-7.456	-0.219827	0.855911
20	43	4.373	2.376	-7.515	0.152219	0.098665
21	44	6.109	2.372	-7.594	0.740077	0.472955
22	45	7.872	2.364	-7.781	0.404407	0.221529
23	46	9.236	2.359	-7.863	0.188145	-1.050864
24	47	10.645	2.337	-7.672	-0.000006	-0.000241
25	51	3.002	1.305	-7.487	0.367114	-0.346675
26	52	4.354	1.308	-7.56	0.165973	-0.380322
27	53	6.107	1.28	-7.59	0.113272	0.543135
28	54	7.867	1.286	-7.887	-0.491814	-0.093516
29	55	9.22	1.263	-7.929	-0.005326	-0.261654
30	61	2.496	0.931	-4.543	-0.076567	0.224698
31	62	3.552	0.368	-4.536	0.612868	0.017973
32	63	4.699	0.365	-4.535	0.155196	-0.479103
33	64	6.033	0.334	-4.657	-0.667894	0.381528
34	65	7.293	0.358	-4.781	-0.035059	-0.100082
35	66	8.588	0.387	-4.591	0.001163	-0.000287
36	67	9.811	0.87	-4.484	0.001023	-0.000119

Table 20. Ground Coordinate Residuals

Point	dx	dy	dz
1	0.008	-0.007	-0.003
2	0.011	0.000	-0.001
3	0.005	-0.013	-0.002
4	-0.014	-0.038	-0.009
5	-0.072	0.015	-0.019
6	0.000	0.002	0.000
7	0.008	0.001	0.000
8	0.009	-0.006	0.000
9	-0.002	-0.018	-0.003
10	-0.018	-0.044	-0.010
11	0.009	0.008	0.053
12	0.012	0.000	0.134
13	-0.009	0.026	0.008
14	-0.002	0.005	0.064
15	0.042	0.016	-0.223
16	0.053	0.002	-0.301
17	-0.057	-0.057	-0.023
18	-0.013	0.014	0.090
19	-0.002	0.006	0.188
20	-0.015	0.015	0.131
21	-0.007	0.011	0.056
22	0.023	0.001	-0.129
23	0.029	-0.003	-0.208
24	-0.038	-0.026	-0.012
25	-0.002	0.015	0.261
26	-0.024	0.013	0.193
27	-0.005	0.004	0.069
28	0.020	-0.006	-0.128
29	0.007	-0.011	-0.164
30	0.098	0.012	0.055
31	0.092	0.019	0.068
32	0.090	0.002	0.068
33	0.109	-0.017	-0.050
34	0.125	-0.030	-0.174
35	0.081	-0.013	0.020
36	0.037	-0.004	0.012
Standard deviation	0.044884	0.018411	0.118218

Table 21 shows that the orientation angles, especially in kappa, of the three frames agree within about 0.01 radians or about 3 minutes. Therefore, they can be constrained in determining location of the roadside features, without any ground control, from sequential video images.

Table 21. Exterior Orientation Elements After Calibration

EXTERIOR ORIENTATION							
PHOTO NO. 1	60	XO	YO	ZO	KAPP(RAD.)	PHI(RAD.)	OMEGA(RAD.)
		5.121502	2.157781	10.680733	-0.012042	-0.050437	-0.090819
STD. ERROR		0.072756	0.073574	0.162008	0.013756	0.005486	0.005174
PHOTO NO. 2	38	XO	YO	ZO	KAPP(RAD.)	PHI(RAD.)	OMEGA(RAD.)
		4.978161	1.985647	3.927138	-0.011833	-0.035009	-0.08509
STD. ERROR		0.045893	0.046128	0.103512	0.013762	0.005481	0.005215
PHOTO NO. 3	25	XO	YO	ZO	KAPP(RAD.)	PHI(RAD.)	OMEGA(RAD.)
		4.948669	1.906532	0.261199	-0.007158	-0.034088	-0.092336
STD. ERROR		0.037508	0.03762	0.077803	0.013753	0.005557	0.005236
WEIGHT		100	100	11.1	0	0	0

In order to test the validity of the calibration, the sequential images from 25 and 60 feet and the stereo pair from 38 feet were processed using Soft Plotter, a commercial software that uses a Silicon Graphics workstation for soft photogrammetric applications. Table 22 gives the standard error of the residual at the control (check) points by photogrammetric triangulation for the three methods using constrained exterior and interior elements from calibration. The results indicate that ground locations can be determined to an accuracy better than 0.25 m. The accuracy of location in *Z*, the direction of travel, is less than those in the *X*, *Y*, which are perpendicular to the direction of travel. Also, the inclusion of the image from 25 feet seems to decrease accuracy. This may be due to the validity of the interior orientation elements as well as the deterioration of the image quality resulting from the imagery that is too close.

Table 22. Error at Checkpoints by Photogrammetric Triangulation

Method	X (m)	Y (m)	Z (m)
Calib with three cameras	0.027	0.024	0.105
SoftPlotter with longitudinal pair	0.067	0.063	0.245
SoftPlotter with stereo pair	0.029	0.037	0.130

Methodology to Determine Position by Video Logging

Three test sites were selected in Story County to evaluate the accuracy of position determination by video logging. Figure 17 shows the test sites: EDM baseline, Grand Avenue, and Nevada.

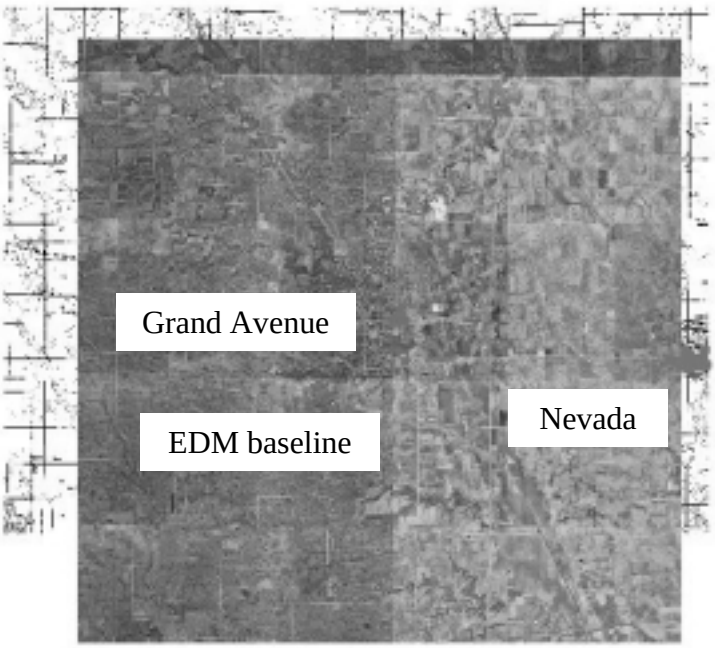

Figure 17. Test Sites (Story County)

EDM baseline (1 mile long) is a rural road; there are five BMs in the right of way with precisely known locations. Total station and RTK GPS as-built surveys were done (see Senthil Kumar, Bhagawati, and Patterson, Real-Time Kinematic GPS Survey, 2001). These surveys were tied to the BM to obtain WGS 84 spherical coordinates and state plane coordinates. Using this information, ArcView-GIS themes were created for comparative studies (see Figure 18). Figure 17 shows that information from topographic maps, orthophotos, and as-built surveys can be analyzed together. Figure 18 shows that as-built surveys and GIS can be used for road maintenance and improvement studies (see Senthil Kumar, Bhagawati, and Patterson, As-Built Surveys and GIS Creation, 2001).

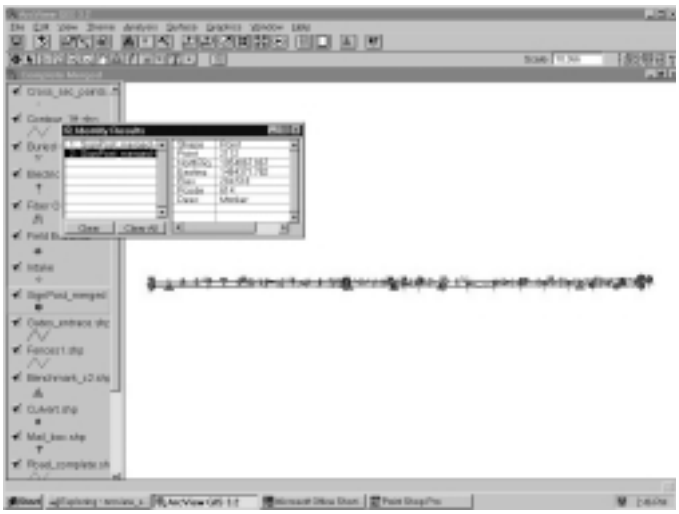

Figure 18. EDM Baseline Theme

Grand Avenue is an urban site including an intersection and an overhead bypass bridge. A total station as-built survey was done on a local coordinate system. A CAD drawing was done using the microstation software, which was then transferred to ArcView GIS themes using 1:24000 USGS topomap as control (see Figures 17 and 19). These themes can then be used to determine geographic and state plane coordinates of any roadside feature and to check the accuracy of the positioning by video logging.

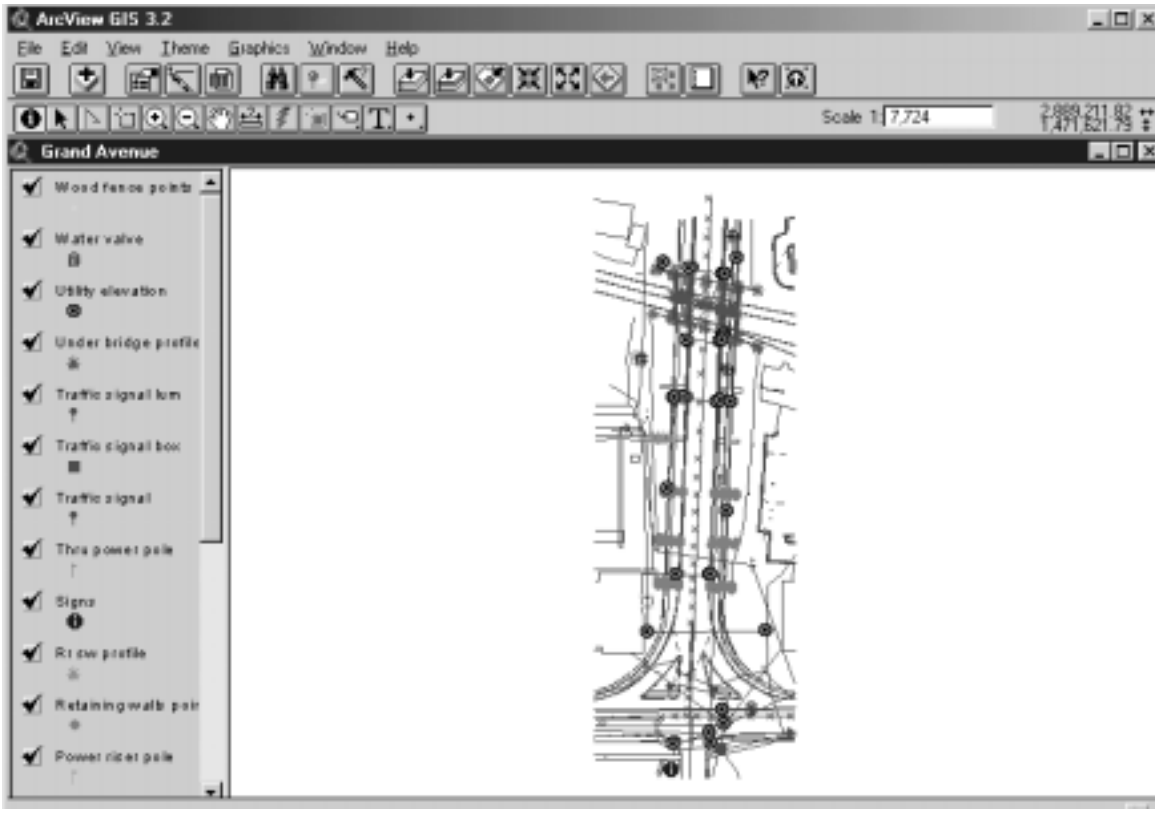

Figure 19. Grand Avenue Theme

The Nevada site is a highway along US 30. As was done in the case of the Grand Avenue site, the CAD files created from the total station survey on a local coordinate system were incorporated into the topographic map theme to get geographic and state plane coordinates of any selected feature (see Figure 20).

Figure 11 shows the features on a video image selected for position determination in the EDM baseline site. Since the video images are taken every 25 feet, by studying their location on sequential images, it is possible to estimate the location of the feature from the camera (Z) within about ±8 feet. From this distance, the scale at the plane of the imagery can be estimated, using the principal distance of the digital camera. The scale can then be used to estimate the perpendicular offsets (X, Y) within about ±8 feet.

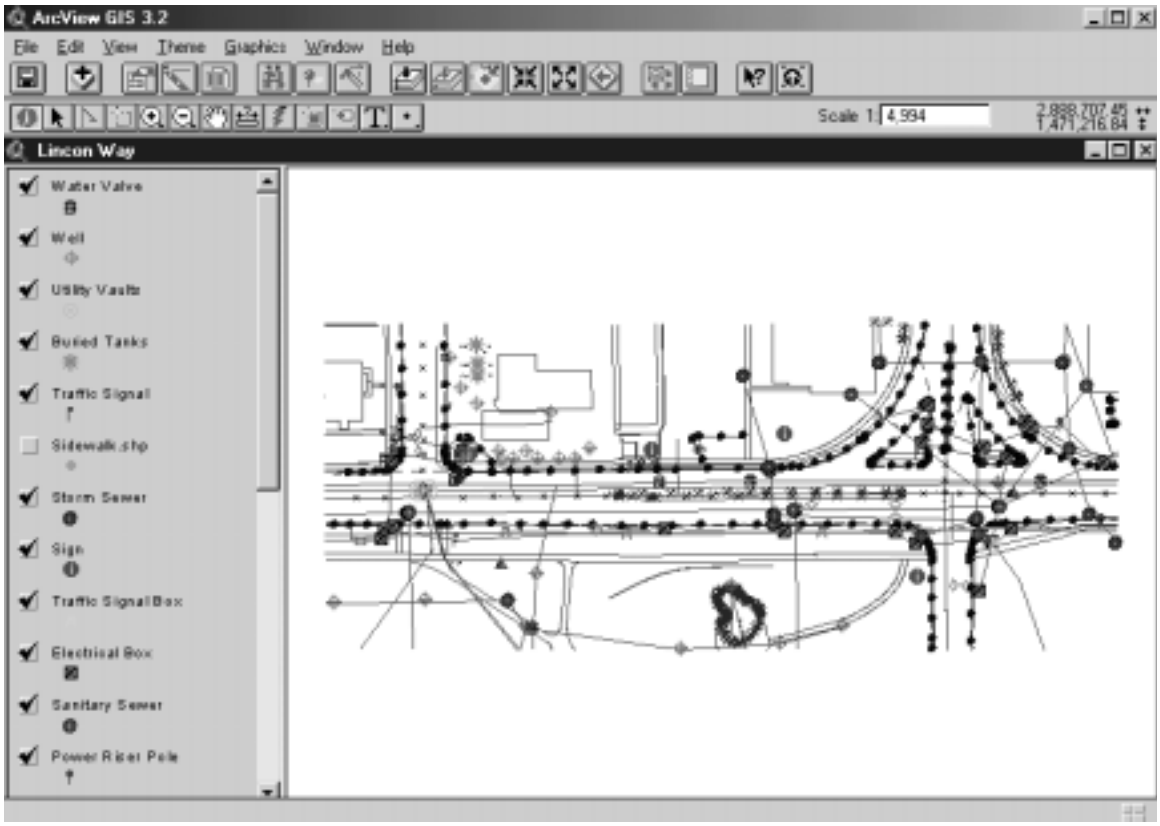

Figure 20. Nevada Theme

The estimated location of a feature can then be used in the Calib or any other soft photogrammetric software to determine its position to an accuracy of ±1 foot using two or more sequential imageries. We found that video images at 100, 75, and 50 feet or 100 and 75 feet from the feature give satisfactory solutions. The camera locations obtained by GPS, the camera orientation angles, and interior orientation elements obtained by prior and or post camera calibration, can be constrained to give satisfactory results without any ground control.

Accuracy Evaluation at EDM Baseline

Table 23 shows the results of the Calib software for two feature locations at the EDM baseline site. The camera interior orientation elements and orientation angles are weighted to the calibrated values. The camera locations are weighted to GPS values with local origin. The standard error of unit weight 6 and photo coordinates residuals less than 0.1 pixels indicate satisfactory results.

Table 23. Feature Location at EDM Baseline

ICYCLE = 3 VARIANCE = 6.15E-00 NDF = 2
CAMERA CALIBRATION OF THE VIDEOLOG F 2000
NO. OF PHOTOS 2
NO. OF CONTROL POINTS 2
DEGREES OF FREEDOM 2
NO. OF CYCLES 3
VARIANCE OF UNIT WEIGHT = 6.15 + 00

RESULTS
INTERIOR ORIENTATION

	X	Y	F						
	0.043355545	0.008555431	-1819.999998						
	K1*1.00E-05	K2*10**-12	K3*10**-18	P1*1.00E-05	P2*10**-12	P3*10**-18			
	-0.000033	-0.000143	-0.000129	0	0	0			
STD ERROR	7.84E-02	7.84E-02	7.84E-02	2.48E-02	2.48E-02	2.48E-02	2.48E-02	2.48E-02	2.48E-02
WEIGHT	1.00E+03	1.00E+03	1.00E+03	1.00E+04	1.00E+04	1.00E+04	1.00E+04	1.00E+04	1.00E+04

EXTERIOR ORIENTATION

PHOTO No	208	XO	YO	ZO	KAPP(RAD.)	PHI(RAD.)	OMEGA(RAD.)
		-0.000902	-0.007504	-2.208767	0.000731	-0.04964	-0.072899
STD.ERROR		0.024783	0.024783	0.024791	0.012037	0.006909	0.007163
WEIGHT		10000	10000	10000	40000	40000	40000

RESIDUALS ON CONTROL POINTS (PHOTO CO-ORDINATE UNITS)

S.NO.	POINT NO.	X - COORD	Y COORD	Z COORD	RES X	RES Y
1	4	-12.005	8.61	-70.925	0.012484	-0.004811
2	40	-9.955	-2.733	-64.207	-0.030666	-0.026487

EXTERIOR ORIENTATION

PHOTO No	2-211	XO	YO	ZO	KAPP(RAD.)	PHI(RAD.)	OMEGA(RAD.)
		-0.054098	0.006448	-26.293321	-0.017957	-0.035691	-0.087495
STD.ERROR		0.024783	0.024783	0.024791	0.01211	0.01053	0.010658
WEIGHT		10000	10000	10000	40000	40000	40000

RESIDUALS ON CONTROL POINTS (PHOTO CO-ORDINATE UNITS)

S.NO.	POINT NO.	X - COORD	Y COORD	Z COORD	RES X	RES Y
1	4	-12.005	8.61	-70.925	0.016894	-0.006483
2	40	-9.955	-2.733	-64.207	0.046823	-0.004

Table 24 shows the accuracy of feature locations by video logging when compared to those obtained from as-built surveys by total station. The direction of travel of the video logging van is in the east direction. Hence, the large error in east coordinate, especially in the west end of the site, is due to systematic error in the camera location determined by GPS and not due to the soft photogrammetric method.

Table 24 shows the error of position determination at the EDM baseline site is better than ± 1 m, if we disregard the systematic error due to camera location in the east coordinate by GPS. The GPS uses the code phase, and therefore, the expected positional accuracy is about ±2 m. This error in GPS could be improved by using the carrier phase. The relative error of ± 1 m in the feature location is satisfactory for most maintenance studies. The accuracy depends on how good the prior estimates of the locations are, especially in *Z*. With repeated runs of the Calib software and using better estimates, more accurate locations can be obtained. One can also determine a number of points from a pair, in which case, since there are no ground control points, any error in the initial estimate of the locations or the measurement of their pixel coordinates of a point tends to affect the accuracy of the other points. Thus, it may be better to do the computation of one point at a time.

Table 24. Error in Positioning by Video Logging (EDM baseline)

Photos	Interval (ft)	D_North (m)	D_East (m)	D_Elev (m)
East end	75	-0.19	0.55	-0.43
East end	100	-0.04	1.35	-0.42
Middle	75	0.29	-0.91	-0.10
Middle	100	0.63	0.34	0.00
West end	75	0.45	3.77	-0.16
West end	100	0.34	3.34	-0.14
Standard deviation	-	0.307293779	1.819413614	0.178077137

Accuracy Evaluation at Grand Avenue

Figure 21 shows the image and the points used to evaluate the accuracy of positioning by video logging in an urban area (Grand Avenue site). In a typical urban road maintenance study, one needs the location of many points on bridges, pavements, sidewalks, etc.

Figure 21. Points Used at Grand Avenue

It is also noted that in this case the gradient of the road is significant and changing. Hence, it is not possible to get accurate location of the camera by kinematic GPS (especially in elevation) to determine the orientation angle accurately. Thus, three or more well-defined points distributed in *x*, *y* common to two or more imageries, must be selected and the Calib software has to be run with good initial estimates of the ground locations to determine the orientation angles and relative ground elevation of the camera. Then, they can be weighted in the Calib software and the locations of points determined one by one similar to the procedure in the EDM site. Table 25 shows that the difference in coordinates obtained from total station and positioning by video logging for two points is less than 0.1 m, which is satisfactory for an urban applications. The

direction of travel by the video van is north and the error is relative and independent of the GPS location.

Table 25. Relative Error in Positioning by Video Logging (Grand Avenue)

Point Description	D_East (m)	D_North (m)
Electric pole	-0.086	-0.035
Road edge	-0.073	0.073

Accuracy Evaluation at Nevada

Figure 22 shows the imagery used at the Nevada site. This is similar to EDM baseline site in which the gradient is small and therefore the orientation angles from calibration site can be weighted with the camera location by GPS in the Calib software to determine the locations of any feature, one at a time. Table 26 shows that the difference in coordinates obtained by total station and video logging is less than 0.5 m, which is satisfactory for highway maintenance applications.

Figure 22. Points at Nevada

Table 26. Error in Positioning by Video Logging (Nevada)

Point Number	Description	D_East (m)	D_North (m)
1	First pole	0.071	-0.090
10	Second pole	0.362	-0.166

Methodology to Locate Roadside Features at Nevada

Video Logging Van with Video Camera and GPS

As part of the as-built survey project, the video logging van was attached with GPS antenna and receiver, and a video camera attached at its front was used to take pictures of various roadside features at a regular interval of 75 feet along US 30 from Ames to Nevada, Iowa. GPS was used to obtain the geodetic positions of the camera positions (see Ramesh, Nevada Project, 2001).

Event Theme

In ArcView, points whose coordinates are known can be imported as an event theme. This requires a test file in which the point name or ID and its location separated by delimiters such as commas are given. The text file is added as a table in ArcView. Then from the view menu of the standard toolbar the text file is added as an event theme with longitude as *X*-coordinate and latitude as *Y*-coordinate. Then the text file can be converted into a shape file using "Convert into shape file" in the theme menu. Thus, the text file containing the GPS positions of the camera points was brought into ArcView as an event theme and converted into shape files. Part of the text file used as an event theme in the project is given in Figure 23.

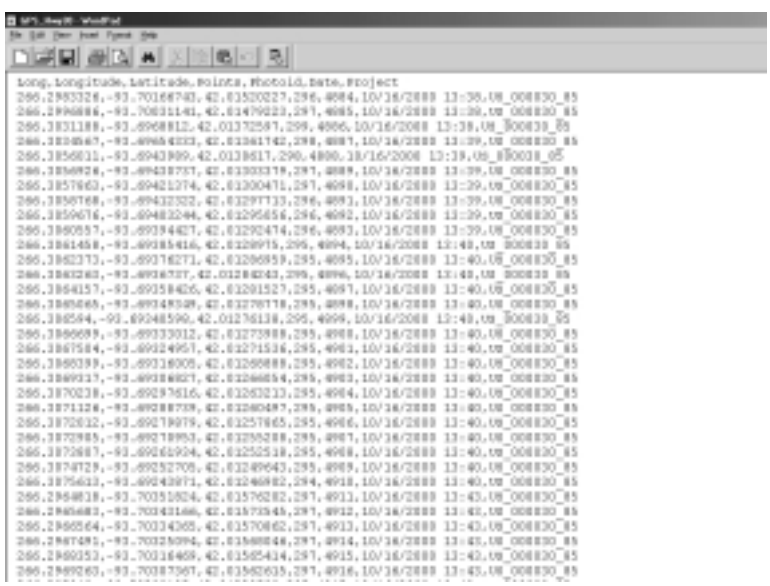

Figure 23. Event Theme Text File

Hotlinks Tool in ArcView

Hotlinks in ArcView is a tool by which the image files can be associated or linked with a particular feature in a theme. Adding a new field in the theme attribute table to have the path of the image file does this. Then in the hotlinks menu of theme properties the newly added field is given as the hotlink field. Thus, the photos or the image files taken from the camera positions were associated with the points using hotlinks in ArcView. See Figure 24.

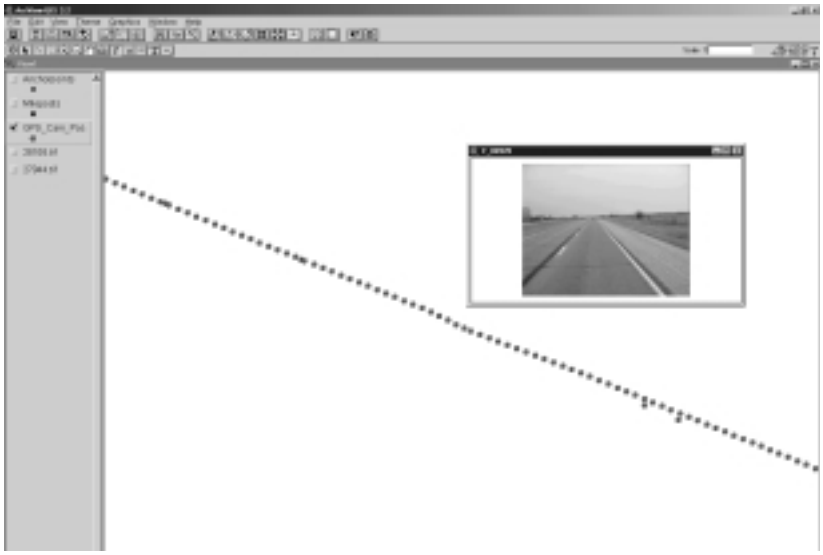

Figure 24. Hotlinks Tool in ArcView

Orthophoto and Topomap

The orthophoto and topomap for the given area were downloaded from the URL www.ortho.gis.iastate.edu in TIFF format. The ArcView header file downloaded along with these images and acted as a world file, helping add the images in ArcView. As the JPG files cannot be viewed in ArcView, an extension called AV-Plus was used.

Location of Mileposts Determination Using Calib Program

For each milepost, the Calib program was used to determine the coordinates of the milepost using two photos, one taken near the milepost and another at about 75 feet behind the first camera position. See Figure 25.

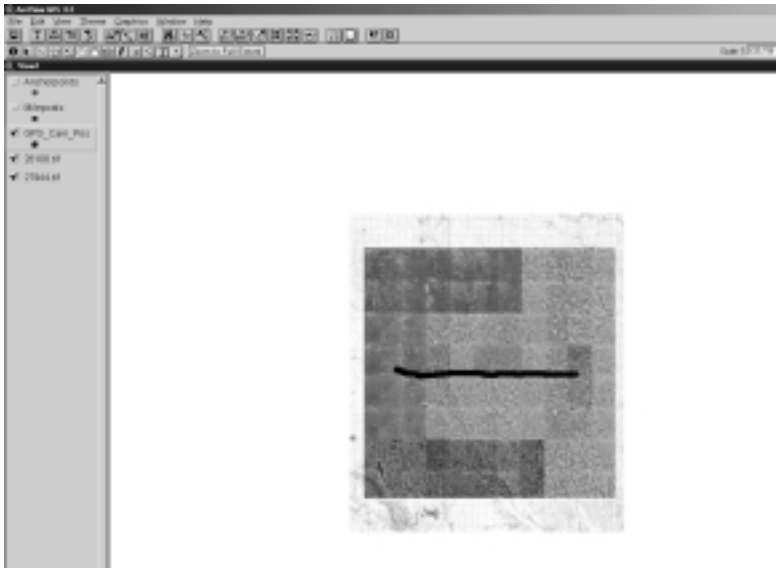

Figure 25. Location of Mileposts Determination Using Calib Program

The camera position of the nearest photo was kept as origin (0, 0, 0). The axis of the local coordinate system was given as follows:

- *X*-axis is positive if the point lies to the right of the principal axis (the line joining the camera positions of a series of photos) and is negative if otherwise.
- *Y*-axis is positive if the point lies above the camera in the van and is negative if the otherwise.
- *Z*-axis is positive if the point lies behind the origin or the camera position of the first photo.

The image coordinates of the mileposts in the two photos were found before going to the Calib program. The format of the image was about 1,030 rows and 1,300 columns. The image coordinates obtained had the origin at the upper left corner of the image. Those image coordinates needed to be transformed so that the origin would be at the center of the image. The new image coordinates were used for the Calib program.

The exterior orientation parameters such as kappa, phi, and omega, obtained from the results of the Calib run of "calibration of camera," were in the Calib.dat. The weight assigned to them was low in order to let them change during the run of the Calib program. The calibration results for each milepost (144, 146, 147, and 149) are given in Ramesh (Nevada Project, 2001).

Transformation Using Transcalib Program

The Transcalib program uses the northing, easting of the camera positions and the *X*, *Z* coordinates of the local system to obtain the northing, easting of the milepost in the state plane

coordinate system. An important point to be noted is that the *X*, *Z* coordinate of local system is the *X*, *Z* coordinate from the exterior orientation results of the Calib program. Thus, using the Transcalib program, the local coordinates were transformed into state plane coordinates.

Sample GPS Survey

A sample GPS survey was carried out on June 19, 2001, for the mileposts 144, 146, 147 and 149 on the Nevada road by positioning the GPS antenna and receiver near the mileposts. The point named "sarath," near the Town Engineering Building at Iowa State University, was used as fixed station.

The GPS data collected were processed using the SOLUTIONS program to obtain the coordinates of the mileposts. When the GPS survey was conducted it was not possible to keep the antenna on top of the mileposts. Therefore, the offsets in the northing and easting directions were noted. Then these offsets were added to the transformed coordinates obtained from the Transcalib program. Then they were compared with the northing and easting obtained from the GPS survey and verified to see if they agreed. The results were compared with the results from the Transcalib program. The compared results are provided in Ramesh (Nevada Project, 2001). The results indicate a systematic error in the easting, the direction of travel. This systematic error is due to the GPS phase code receiver of the video logging van, which can be eliminated by having checkpoints every 10–15 miles. After eliminating this systematic error the standard error of the position determination was less than 2 m.

Triangulation Using SoftPlotter

SoftPlotter 1.6 was used for triangulation process with the mileposts and other points distinct enough and common in both photos. To start, a new project was created. Video logging camera parameters such as *X*, *Y*, *F*, K1, K2, K3, P1, P2, and P3 were done in the camera editor of the block tool. Then the two photos were imported in the imagine format (i.e., *.img) in the frame editor of the block tool. Then *Xo*, *Yo*, *Zo* from Calib.dat and kappa, phi, and omega and their corresponding sigma were provided from the Calib results. Then it was applied and exited. In the ground point editor, the milepost was given as a control point. The *X*-coordinate, *Y*-coordinate, and *Z*-coordinate were obtained from the results of the Calib program.

Then in the ground point editor, the *X*, *Y*, *Z* coordinates of the known ground points were given along with the weights assigned to them according to their accuracy. We needed at least three horizontal control points and two vertical control points for triangulation to be carried out.

Interior orientation was the next process. It was selected from the activities menu of the block tool. Interior orientation is usually done by clicking the fiducials on the photo corresponding to the fiducials of the camera. The interior orientation was obtained for each photo one by one. The RMS error IDs verified to be within the tolerance limit.

Then came the ground point measurement selected from the activities menu of the block tool. In this step, the two frames were viewed in two different panels, and clicking the same point on the two frames and then clicking the button “Take measurement” took the measurement of a point. Care needed to be taken so that the same point was viewed before taking the measurement.

Now the triangulation was done with the convergence value around 0.03 and maximum to be 10. The triangulation results (see Ramesh, Nevada Project, 2001) were viewed and checked for the error using the point and image residuals.

Northing, Easting, and Elevations of Mileposts and Anchor Points

Four parameter transformation equations were used for getting the northing, easting, and elevations of the mileposts. A four-parameter transformation equation was used because the origins of the two coordinate systems were not the same; therefore, translation needed to be done in addition to rotation and a scale change. Thus, the equations used were as follows:

$$X2 = a\,X1 + b\,Y1 + c$$
$$Y2 = -b\,X1 + a\,Y1 + d$$

or

$$\begin{bmatrix} X2 \\ Y2 \end{bmatrix} = \begin{bmatrix} a & b \\ -b & a \end{bmatrix} \begin{bmatrix} X1 \\ Y1 \end{bmatrix} + \begin{bmatrix} c \\ d \end{bmatrix} .$$

The above transformation is usually referred to by one of the many names: a two-dimensional linear conformal transformation or a two-dimensional similarity transformation.

While finding the northing and easting of the mileposts, Z and X of the local coordinates system were used and transformed. For finding the elevation, Z and Y of the local coordinate system were used to be transformed into easting and elevation of the mileposts.

In the four-parameter transformation, there were four unknowns a, b, c, and d. In order to find these parameters, four equations were needed. From a single point we got two equations. Therefore two points were needed to solve for a, b, c, and d. Thus the two camera positions for each mileposts were used to solve for a, b, c, and d.

The equations used for finding the northing and easting of the mileposts were as follows:

$$\text{northing} = a\,Z + b\,X + c$$
$$\text{easting} = -b\,Z + a\,X + d$$

First the northing and easting of the two camera positions were used to solve for *a*, *b*, *c*, and *d*. Then the values of *a*, *b*, *c*, and *d* were used to find the northing and easting of the mileposts. The positive values of *Z* and *X* were used.

For finding easting and elevation of the mileposts, the following equations were used:

$$\text{easting} = a\,Z + b\,Y + c$$
$$\text{elevation} = -b\,Z + a\,Y + d$$

Here the negative of *Z* is used in place of *Z*.

Then the results for northing and easting of the mileposts were compared with the northing and easting of mileposts obtained from the Transcalib program. It was found that the results from Transcalib program were very much closer to the values obtained from GPS survey. So the northing and easting obtained from Transcalib were used as the northing and easting of the mileposts. But the results of elevation obtained from the four-parameter transformation were found to be closer to the values from GPS survey. Therefore, those elevation values were used as the elevation of the mileposts. The transformation equation matrix of northing and easting, easting and elevation, and subsequent calculations to determine the location of anchor points and mileposts are given in Ramesh (Nevada Project, 2001). The results of the 14 mileposts found at the Nevada road are given in Table 27.

Table 27. Nevada Mileposts

Mileposts	Northing	Easting	Elevation
144	1056945.671	1484010.721	290.939
145	1056350.159	1485496.586	284.184
146	1056289.264	1487119.280	272.372
147	1055857.841	1488608.255	266.919
148	1056008.482	1490209.425	249.624
149	1056157.276	1491810.080	245.186
151	1056318.771	1493559.164	247.252
152	1056466.561	1495133.064	263.478
153	1056500.910	1496735.498	268.560
154	1056504.133	1498342.607	269.560
155	1056491.499	1499952.214	271.560
156	1056477.928	1501580.317	278.300
157	1056202.25	1503168.069	275.534
158	1056218.481	1504764.369	281.773
159	1056409.062	1506336.848	276.726
160	1056394.832	1507947.126	280.557
161	1056375.983	1509546.681	268.492
162	1056409.738	1511155.982	283.453
163	1056456.717	1512765.309	284.598
164	1056452.145	1514371.948	290.600
165	1056385.140	1515996.714	294.894

Mileposts locations were then brought into ArcView-GIS as an event theme. In ArcView project newroad.apr, other themes such as GPS camera positions, orthophoto image, and topomap were in the UTM coordinate system. Hence, the mileposts point theme was projected from state plane system to UTM system and then added as a theme in the project. See Figure 26.

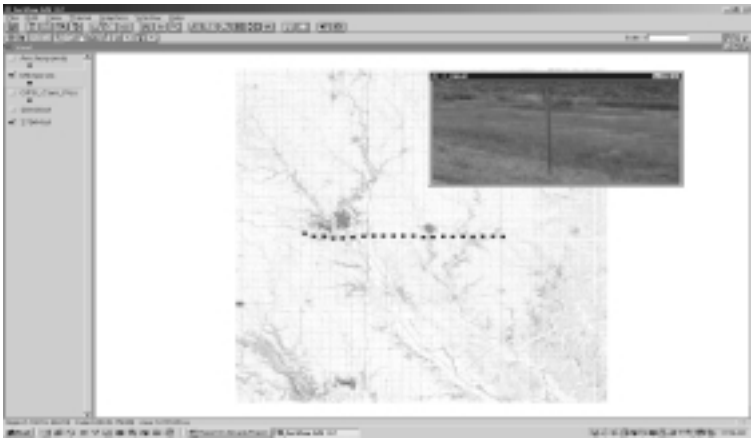

Figure 26. ArcView Project

Similarly, the northing, easting, and elevation of the 10 anchor points were also determined and added as a separate theme in the ArcView. The results of the Anchor points are given in Table 28.

Table 28. Anchor Point Results

Points	Northing	Easting	Elevation
US 69 point 1	1056017.163	1490221.448	250.312
US 69 point 2	1056018.147	1490222.145	250.167
US 69 point 3	1056020.364	1490223.302	249.870
Junction point	1056489.823	1501473.595	275.615
Nevada bridge point 1	1056135.133	1504068.572	265.543
Nevada bridge point 2	1056136.651	1504071.843	265.204
Nevada exit point 1	1056394.023	1505280.249	279.741
Nevada exit point 2	1056390.912	1505279.195	280.011
Far bridge point 1	1056375.341	1510225.655	274.307
Far bridge point 2	1056377.547	1510225.72	274.094

Figure 27 shows the anchor points added as a separate theme in ArcView. The figure also shows the mileposts and topomap.

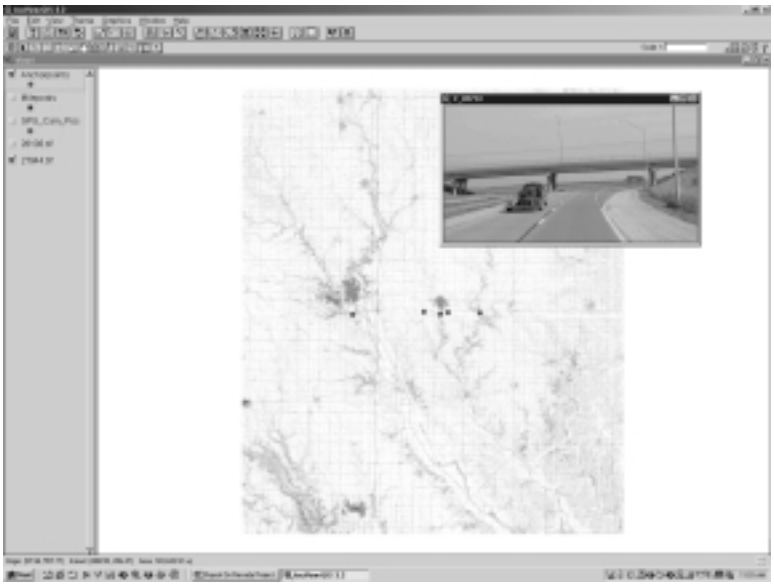

Figure 27. Anchor Points Added as a Separate Theme in ArcView

Thus, the mileposts, anchor points, and camera positions are brought into ArcView for further analysis. These coordinates will have systematic errors due to the code Phase GPS, which depends on its distance from the base station, etc. This systematic error can be eliminated using control points every 10–15 miles established by the static GPS carrier phase method.

Position Determination Conclusions and Recommendations

Location of roadside features can be determined by photogrammetric methods from video imageries obtained from a van equipped with a video camera, GPS, and INS. The accuracy depends on the accuracy of the GPS system. The GPS system used in this study uses a P-code phase system, and therefore the expected accuracy is about ±2 m. The video camera has to be calibrated in dynamic mode using a three-dimensional calibration range. The position can be determined from sequential imageries; there is no need for stereo imageries. Software that can be used for calibration and triangulation, such as Calib, is available in the market. The initial estimate of the distance from the camera to the feature along the direction of travel, *Z*, is critical in determining an accurate position. Using sequential imageries controlled by an INS estimate of *Z* can de done satisfactorily. The coordinates determined have to be corrected for any systematic error caused by the GPS code phase system by having a control point every 15 miles

The location of roadside features can be used to locate mileposts and anchor points and to create two-dimensional GIS, three-dimensional GIS, and virtual roads. This involves collecting a large quantity of data; thus, it is recommended that research be done to automatically identify and locate selected features and to create a database useful for safety studies or maintenance and GIS applications.

Since the global positioning system is critical, it is recommend that the Iowa DOT's Video logging system be updated to use the kinematic L1 and L2 carrier phase system, which should give locations within ±10 cm accuracy.

CONCLUSIONS AND RECOMMENDATIONS

This research involved two studies: one to determine the local geoid to obtain m.s.l. elevations from a GPS to an accuracy of ±2 cm, and the other to determine the location of roadside features such as mile posts, stop signs, etc., for safety studies, GIS, and maintenance applications, from video imageries collected by a van traveling at traffic speed.

Four phases of local geoid determinations were conducted for nine stations in Story County. The local geoid variation fluctuated with time, and the mean of the first three had standard errors of less than ±2 cm with the fourth. It was noted that the variations in local geoid may be due to motion of the axis of rotation of the earth. A need for a fixed-height antenna for all stations was indicated. It was also found that two sessions of observation can be used to detect blunders. The mean of the last three phases local geoid undulation can be used to correct GPS observations for the next two years. It is recommended that the variation of local geoid over a long period of time, about 4–18 years, be studied so as to determine the validity of the moving average.

A video logging van captured imageries at three test sites: Grand Avenue, an urban site; EDM baseline, a rural site; and US 30 in Nevada, a freeway, at 55 mph. The video camera has to be calibrated using a three-dimensional calibration range and photogrammetric calibration software. Sequential imageries can then be used to determine locations on a local coordinate system without any control by constraining the interior and exterior orientation elements from calibration. The local coordinates can then be transformed to state plane coordinates using the camera locations determined by GPS. Evaluation of the data showed that the roadside feature location can be determined with relative accuracy better than 10 cm and absolute accuracy of ±2 m, depending on the global positioning system. The coordinates determined have to be corrected for any systematic error caused by the GPS code phase system by having a control point every 15 miles. The method developed was used to determine the state plane coordinates of mileposts and anchor points located along a 14-mile portion of US 30 from Ames to Nevada, Iowa. This information can be used in GIS and maintenance applications, as well as in safety studies. It is recommended that the Iowa DOT update the video logging van with a kinematic carrier phase GPS and conduct research for automatic data capture and creating virtual roads.

It is recommended, as suggested by the steering committee, that the results of this research be presented at local, national, and international meetings.

ACKNOWLEDGMENTS

The authors wish to thank the Iowa Highway Research Board and the Iowa Department of Transportation for supporting this research. Special thanks goes to Mark Dunn, Iowa DOT research engineer and IHRB executive secretary, for his support from the inception to the completion of the project. Thanks are due to Ian MacGillivray of the Iowa DOT for his assistance in selecting the steering committee. Thanks are due to the members of the steering committee—Bruce Brakke, Don Callender, Sara Flanagan, Greg Parker, Bill Schuman, John Smythe, Alice Welch, John Whited, and Jim Witt—for establishing the work plan to complete this project. Special thanks are due to John Whited for selecting the Nevada project and assisting in obtaining the necessary data.

Dennis O'Brien and his staff together with Norm Miller and his staff at the Iowa DOT selected the benchmarks, performed three-wire leveling wherever necessary, and collected the GPS data for all four phases. Sheri Anderson and her staff at the Iowa DOT collected all the video images used in this project. Our thanks go to all of them. Special thanks are due to Dennis O'Brien for his enthusiasm and keen interest in this research.

Thanks are due to Steve Andrle and his staff at the Center for Transportation Research and Education, Iowa State University, for all their assistance in getting this project completed in time. Special thanks goes to Mark Anderson-Wilk of CTRE in editing the reports generated in this project. Thanks are due to Lowell Greimann and his staff at the Department of Civil and Construction Engineering, ISU, as well as to the Iowa State administration in providing the facilities, computer, and moral support to conduct this research as well as the graduate students involved in the study.

Last but not least, this research could not have been conducted if not for the tireless work done by the students engaged in this project. Special thanks go to Dwipen Bhagawati, Ph.D., P.K. Senthil Kumar, M.S., Cynthia Patterson, M.S., Ruifeng Xi, Ph.D. (pending), A.C. Ramesh, M.S. (pending), Steve Deiness, Ph.D. (pending), and Eric Langley, B.S. (pending).

REFERENCES

Bhagawati, D., and C. Patterson. *Dynamic Calibration: Internal Report.* Iowa State University, Ames, Iowa, 2001.

Bhagawati, D., and C. Patterson. *Feature Determination: Internal Report.* Iowa State University, Ames, Iowa, 2001.

Cederholm, P. Integrating GPS with Dead Reckoning Sensors. *Surveying and Land Information Systems,* Vol. 60, No. 4, 2000, pp. 259–266.

Jeyapalan, K., et al. *Maximized Utility of the Global Positioning System: Final Report.* Project HR-316. Iowa Department of Transportation and Iowa Highway Research Board, Ames, Iowa, 1991.

Jeyapalan, K., et al. *Soft Photogrammetry for Highway Engineering: Final Report.* Project HR-387. Iowa Department of Transportation and Iowa Highway Research Board, Ames, Iowa, 1998.

Ramesh, A.C. *Geoid 282-01 (Phase III): Internal Report.* Iowa State University, Ames, Iowa, 2001.

Ramesh, A.C. *Geoid 78-02 (Phase IV): Internal Report.* Iowa State University, Ames, Iowa, 2002.

Ramesh, A.C. *Report on Nevada Project: Internal Report.* Iowa State University, Ames, Iowa, 2001.

Senthil Kumar, P.K., D. Bhagawati, and C. Patterson. *As-Built Surveys and GIS Creation: Internal Report.* Iowa State University, Ames, Iowa, 2001.

Senthil Kumar, P.K., D. Bhagawati, and C. Patterson. *Real-Time Kinematic GPS Survey: Internal Report.* Iowa State University, Ames, Iowa, 2001.

Senthil Kumar, P.K., and C. Patterson. *Local Geoid Determination Phase I: Internal Report.* Iowa State University, Ames, Iowa, 2001.

Senthil Kumar, P.K., and C. Patterson. *Local Geoid Determination Phase II: Internal Report.* Iowa State University, Ames, Iowa, 2001.

Torge, Wolfgang. *Geodesy.* Walter de Gruyter, New York, 1991.

APPENDIX A: PLAN FOR DEVELOPING LOCAL GEOID

Geoid with sufficient accuracy is required to use differential GPS (DGPS) to obtain m.s.l. elevation. As indicated by the HARN project, global geoid determined by NGS using gravity data gives a maximum error of ±30 cm in the state of Iowa. However, an accuracy of about ±2 cm is required for elevation control in preliminary surveys and orthophoto mapping. It is believed that a local geoid for a countywide area with an accuracy of ±2 cm could be developed. The tasks for this work plan are as follows:

Task 1	Locate eight to nine benchmarks in Story County with reliable NAVD 88 elevations and suitable for GPS observations.
Task 2	Check the reliability of elevation, the duration of GPS data collection, the effects of temperature, pressure, humidity and ionosphere in GPS data processing, the number of sessions needed (at least two), and period of observations required for each session (at least two hours).
Task 3	Simultaneously collect GPS data at the selected BMs in September/October 2000.
Task 4	Process the data using different software packages and conditions. Analyze the results and create a temporary geoid model.
Task 5	Simultaneously collect GPS data at the same BMs again in March/April 2001. Repeated measurements are to check the validity of the model and to filter any change in the geoid with time.
Task 6	Process the data using different software packages and conditions. Analyze the results.
Task 7	Develop the local geoid using the first year observations.
Task 8	Prepare preliminary and progress report. Present report to the Iowa Highway Research Board.
Task 9	Prepare instructions for developing local geoid in any other county and assist in selecting suitable BMs for geoid determination for a selected county.
Task 10	Simultaneously collect GPS data again at the same story county BMs in September/October 2001.
Task 11	Process the data using different software packages and conditions. Analyze the results for any change in the local geoid.
Task 12	Simultaneously collect GPS data again at the same BMs in March/April 2002.

Task 13 Process the data using different software and conditions. Analyze the results. Finalize the local geoid model for Story County.

Task 14 (a) Prepare and present papers at national and local meetings. (b) Prepare and present final report to the Iowa Highway research Board.

APPENDIX B: PLAN FOR DEVELOPING OR SELECTING USER-FRIENDLY POSITIONING

In the past few years video logging of roadside features has been an accepted procedure for verifying such features. Unfortunately, users do not implement it for locating roadside features and mapping at 1″ = 100′ or better. It is believed that soft photogrammetric methods can be used to determine *X*, *Y*, *Z* locations using sequential video images from a digital camera mounted on a moving vehicle whose positions are determined by DGPS. The tasks for position determination by video logging are as follows:

Task 1 Select three sites. The sites used for this study should satisfy the following conditions. They should

(a) be suitable to connect the HARN network with ±5 cm accuracy
(b) be suitable for video logging
(c) include a rural road for plan, profile, and cross-section survey at 1″ = 100′ preliminary survey
(d) include a bridge for maintenance study at 1″ = 10′
(e) include an intersection for traffic study at 1″ = 10′
(f) have projects separated by about 5–10 miles so as to demonstrate the capability to connect them with absolute accuracy of about ±10 cm (1″ = 100′)
(g) include an urban area with obstruction by trees and buildings for mapping at 1″ = 25′
(h) include a residential area as well as a highway with four lanes for an as-built survey at 1″ = 50′ scale

The work plan for this task is to initially select three to five sites in Ames and Nevada area, video the sites, and then select the final three sites.

Task 2 Collect data by total station and RTK. The relative accuracy required for a 1″ = 10′ as-built survey is ±0.2′ or ±5 cm. Thus, the control for this survey has to be at least accurate to about ±3 cm. Total station methods are well established for collecting data at relative accuracy of ±0.2′, and DGPS are well established for control in *X*, *Y* at ±3 cm accuracy. RTK is not very well established for collecting accurate line features, etc., required in as-built surveying. Note that the RTK system is currently used by the Iowa DOT for R.O.W. surveying. The work plan for this task is to

(a) establish control points by DGPS survey to each test site
(b) collect data by total station in each test site
(c) collect RTK data by RTK system in the rural site and compare accuracy, cost, and time. Two types of RTK systems will be used: “back pack” for collecting point features and “vehicle” system for line features, such as edge of a road, etc.
(d) create AutoCAD/microstation files for all sites

Task 3 Create GIS files for roadside features for evaluation of the video logging. It appears there are three common GIS used by the Iowa community involved with roadside features: Arc/Info, Integraph, and MapInfo. ISU's Department of Civil and Construction Engineering has ArcInfo capabilities, CTRE has MapInfo capabilities, and the Iowa DOT has Integraph capabilities. Initially we will use ArcInfo. Then if sufficient interest exists, we will also use the other systems with the help of CTRE and Iowa DOT personnel. The work plan for this task is to

(a) convert all AutoCAD/Microstation files to ArcView files
(b) using the Federal Highway Administration (FHWA) study survey results, create tables for each feature
(c) collect additional field data to complete the feature tables such as heights of signposts, power poles, traffic signs, etc.
(d) combine all three sites into one system on a scale of 1″ = 100′ using the state plane coordinate system and check absolute accuracies between sites
(e) select examples of spatial analysis and develop "AML" or script for decision making (e.g., line of sight and degree of curve)

Task 4 Study the image characteristics such as IFOV and depth of focus of the Iowa DOT video logging system. A test with roadside features set at various distances (25, 50, and 100 feet) will be videoed and evaluated.

Task 5 Design a calibration range to study the geometric characteristics of the digital camera and give interior orientation elements (x_o, y_o, f, K_1, K_2, K_3, P_1, P_2, P_3) with reliability. Test site with about 30 targets separated in X, Y to cover the format, as well as in Z to cover the depth, will be established, and the digital camera will be calibrated.

Task 6 Calibrate the camera and the GPS set up of the video logging van using the calibration range and analyze the results.

Task 7 Test site 1 will be video logged using the Iowa DOT video logging system to check the accuracy of the DGPS of the van and the position determination by soft photogrammetry.

Task 8 Test site 2 (urban area) will be video logged to check the accuracy of bridging video images by soft photogrammetry to give position locations of the camera where intermittent GPS lock is lost due to obstruction by trees, buildings, etc.

Task 9 Test site 3 will be video logged to check the accuracy of integrating video images from multiple passes at high speed. It is expected that we will have four passes along the Highway 30 at 55 mph.

Task 10 Prepare and present preliminary and progress report to Iowa Highway Research Board.

Task 11 Study the 12-mile LRS project in Nevada, Iowa, to determine the anchor point location by video logging and soft photogrammetry.

Task 12 Collect and process data for the LRS project and determine the anchor point locations with an accuracy better than 2 m.

Task 13 Prepare final report and present results in local and national meetings.

APPENDIX C: INSTRUCTIONS FOR ESTABLISHING ELEVATION CONTROL BY GPS FOR REAL-TIME KINEMATIC GPS SURVEYS

In real-time kinematic GPS surveys, most manufacturers use elevation control points and polynomials to correct for geoid undulation in an area less than 3 miles from the base station. The polynomials used depend on the number of available control points. Typically the polynomials used are

$$G = Ax^2 + By^2 + Cxy + Dx + Ey + F ,$$

where G is the geoid undulation correction; A, B, C, D, E, and F are the parameters; and x, y are the latitude, longitude or state plane or local coordinates.

Thus, if only one control is available, then only the parameter F is determined and used for the area. If six or more controls are available and evenly distributed, then all the parameters are determined and used to determine the elevation of any point in the area by calibrating the RTK GPS receivers for that setup. Every time the base station is revisited, the receivers have to be calibrated using the control points as the parameters may change.

In practice, elevation control points with at least third-order accuracy are not easily available for an RTK project area. However, a number of BMs with third-order or better accuracy are available in a countywide area, and possibly one of them is connected to the HARN. These stations can be used to determine the local geoid for the county and then used to establish elevation control for the RTK project area. See Figure C.1.

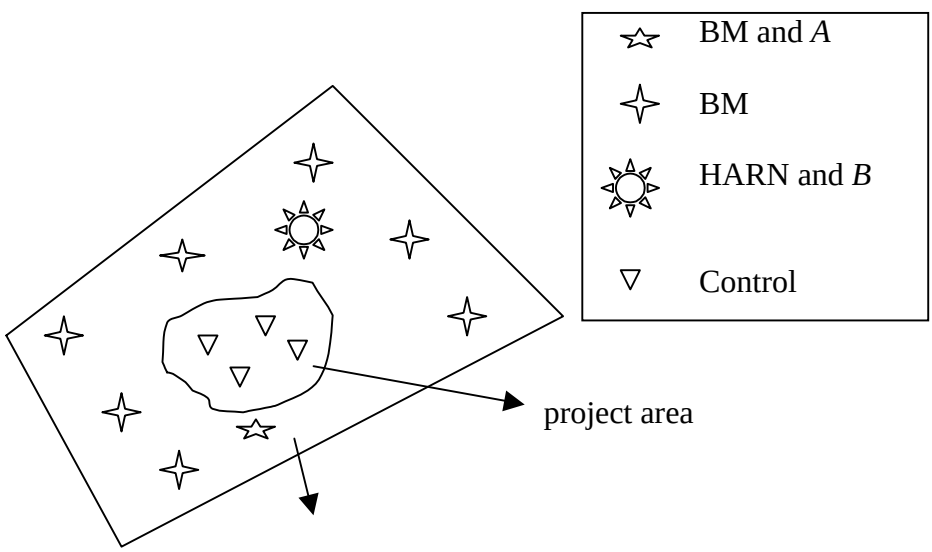

Figure C.1. Using Bench Marks in a Countywide Area

Establishing elevation control by GPS for a RTK project involves nine steps:

1. Select eight or more BMs whose elevations are known with third-order or better accuracy within the county wide area. The points have to be evenly distributed so that the local geoid contours interpolated using the values at these points will represent the area. See Figure C.1. The maximum deviation of the local geoid undulation should be less than 10 cm; if more than 10 cm, then the area has to be divided into two or more sections. An estimate of the local deviations for the area can be made by analyzing the residuals at the vertical control points in the HARN adjustment.

2. If any one of the BMs is not a HARN point, then select a HARN point within or near the area. The HARN point can be used to determine the latitude and longitude locations of the BM.

3. Simultaneously collect about 4 hours GPS data for a window with P-DOP better than 5. Repeat this observation for another 4 hours for detecting blunders. If a blunder is detected in a vector, then that vector has to be reobserved.

4. The GPS data have to be processed one vector at a time from a station close to the project, say *A*, and the local geoid, N_L, at each point, which is the difference between the known MSL elevation and GPS-determined elevation after applying the global geoid correction, N_G, is determined. See Figure C.2 and Table C.1.

   $\pm N_L$ = MSL elevation – (GPS elevation – N_G)

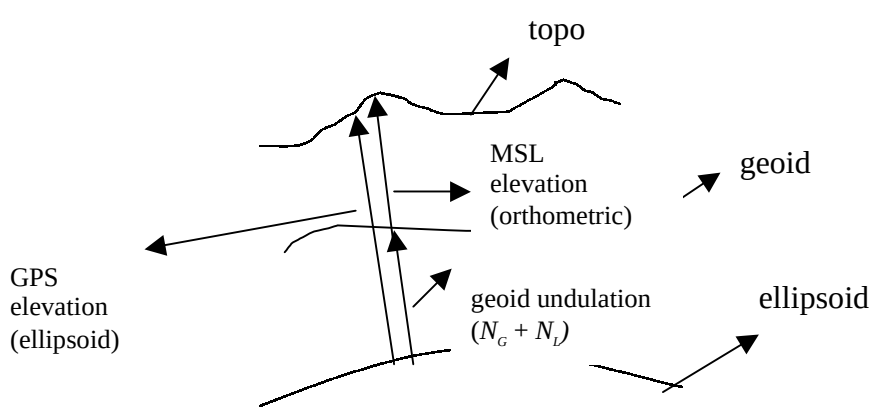

Figure C.2. Determining Local Geoid

Table C.1. N_L

Station	Latitude	Longitude	GPS Elevation (Ellipsoid)	Published MSL Elevation (Orthometric)	N_G	N_L = MSL – GPS + N_G
DOT	42.02224017	-93.62223558	263.742	292.749	-29.35	-0.343

The GPS elevation of BM *A* can be approximately assumed as the known MSL elevation corrected with N_G or can be determined from the GPS elevation of the HARN station:

GPS elevation ≅ MSL elevation + N_G

5. As mentioned in step 1, the maximum deviation of the local geoid undulation should be less than 10 cm; if more than 10 cm, then the area has to be divided into two or more sections. Using the local geoid and the coordinates such as latitude, longitude, or state plane coordinates (N, E) at each of the BMs, a local geoid contour, GRID or TIN, for the station A, is created using the standard contour programs. Figure C.3 shows the local geoid contours, and Table C.2 shows the table for creating contours.

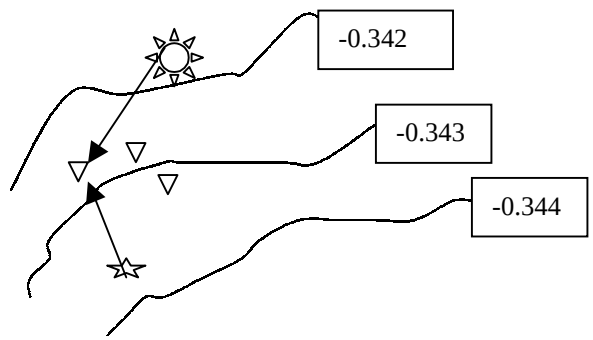

Figure C.3. Local Geoid Contours

Table C.2. Creating Contours

Station	Latitude (y or N)	Longitude (x or E)	GPS Elevation	N_L (Day 78-02 - A)
DOT	42.02224017	-93.62223558	263.742	-0.343
G601	42.16613117	-93.34671659	299.865	-0.302
G499	41.87752236	-93.40988224	232.265	-0.344
G605	41.8982747	-93.52877836	234.075	-0.272
G301	41.99380184	-93.69764569	285.494	-0.36
G117	42.02261136	-93.41862877	277.521	-0.295
G501	42.00801659	-93.47753102	273.798	-0.347
G001	42.02991643	-93.65240797	264.456	-0.351
G506	42.02694027	-93.64533995	258.292	-0.361
G017	42.00522844	-93.44682404	269.959	-0.425

6. Within 6 months of step 3 using the station A as the known station, the MSL elevation of elevation control points for a RTK project can be established by static GPS observation. The GPS observation gives the GPS elevation and the MSL elevation is then computed from

MSL elevation = GPS elevation - $N_G \pm N_L$.

The global geoid N_G is determined using NGS software, and N_L is determined from the local geoid contour, GRID or TIN (see Figure C.3 and Table C.3)

Table C.3. MSL Elevation

Station	Latitude	Longitude	GPS Elevation	N_G	N_L	MSL Elevation =GPS – N_G + N_L
X	42.01883993	-93.62499872	244.119	-29.35	-0.343	273.126

7. It is recommended that steps 4, 5, and 6 be repeated for another station, say B; then the MSL elevation for control points determined from station A can be checked for blunders. The difference between the two can be used to estimate the accuracy of the MSL elevation determined. The weighted mean from A and B will be 1.5 times better than that from A alone.

8. If step 6 is done six months after steps 3, 4, and 5, then these steps have to be repeated every 6months to compensate for the movement of the earth's axis of rotation. However, after four such repeated observations, the steps 3, 4, and 5 are repeated once every 2 years and the moving average of the last three observations can be used in step 6.

9. The control points established in step 6 are equivalent to a third-order BM and can then be used for years to come provided the points are properly constructed like a normal BM with about a 5-foot-long rebar surrounded by 3 to 6 inches of concrete so as to prevent both horizontal and vertical movement. These elevation controls can be used to control both RTK survey project as well as a leveling project.